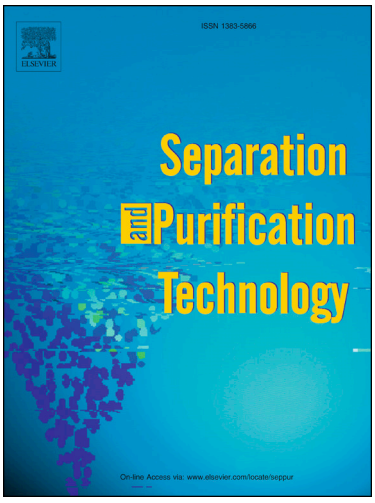

Fabrication, Tuning and Optimization of Poly (acrilonitryle) Nanofiltration Membranes for Effective Nickel and Chromium Removal from Electroplating Wastewater

Seyed Saeid Hosseini, Azadeh Nazif, Mohammad Amin Alaei Shahmirzadi, Inmaculada Ortiz

PII: S1383-5866(17)30867-5
DOI: http://dx.doi.org/10.1016/j.seppur.2017.06.018
Reference: SEPPUR 13796

To appear in: *Separation and Purification Technology*

Received Date: 18 March 2017
Revised Date: 7 June 2017
Accepted Date: 8 June 2017

Please cite this article as: S. Saeid Hosseini, A. Nazif, M. Amin Alaei Shahmirzadi, I. Ortiz, Fabrication, Tuning and Optimization of Poly (acrilonitryle) Nanofiltration Membranes for Effective Nickel and Chromium Removal from Electroplating Wastewater, *Separation and Purification Technology* (2017), doi: http://dx.doi.org/10.1016/j.seppur.2017.06.018

Fabrication, Tuning and Optimization of Poly (acrilonitryle) Nanofiltration Membranes for Effective Nickel and Chromium Removal from Electroplating Wastewater

Seyed Saeid Hosseini[a*], Azadeh Nazif[a], Mohammad Amin Alaei Shahmirzadi[a], Inmaculada Ortiz[b]
[a] Department of Chemical Engineering, Tarbiat Modares University
Tehran, 14115-114, Iran
[b] Department of Chemical and Biomolecular Engineering, Universidad de Cantabria
39005 Santander, Spain
* saeid.hosseini@modares.ac.ir

Abstract

In the present study, response surface methodology (RSM) is employed according to central composite design (CCD) for modeling and optimization NF membranes fabricated and tuned for effective removal of Ni and Cr from electroplating wastewater streams. The effect of concentration of poly(acrylonitrile) (PAN: 21-25 wt. %) as the main membrane material as well as poly(ethylene glycol) (PEG: 0-1.5 wt. %) and titanium dioxide nanoparticles (TiO_2: 0-1 wt. %) as the additives and their mutual interaction on membrane performance and morphology were investigated. According to the quadratic polynomial model, independent factors were statistically significant and the obtained models were accurate. The optimized responses for Ni and Cr rejection and pure water flux were 87.093 (%), 83.271 (%) and 71.801 ($Lit.m^{-2}.h^{-1}$) respectively at optimum membrane formulations of PAN: 23.93%, PEG: 0.41% and TiO_2: 0.82%. The results of validation experiment confirm the data for predicted model at optimum point (Ni rejection: 88.093 %, Cr rejection: 80.271 % and pure water flux: 76.801 $Lit.m^{-2}.h^{-1}$). Both Ni and Cr rejections increased from 60.87% to 80.36% and from 56.35% to 78.64 %, respectively upon increasing PAN concentration in the dope from 21 wt.% to 25 wt.%. It was also found that decreasing PEG concentration led to increase in Ni and Cr rejections and decrease in pure water flux. Using of TiO_2 nanoparticles led to increase of Ni and Cr rejections and pure water flux at different PAN concentrations. From the morphological perspective, increase in polymer concentration led to change of porous to spongy like structure while increasing PEG concentration led to increase in macrovoids area. Both porosity and mean pore size reduced by increase of PAN concentration and decrease of PEG concentration.

Keyword: Nanofiltration membrane, Nickel & Chromium, Electroplating wastewater, Statistical analysis, Optimization.

1. Introduction

Electroplating is one of the most widely used techniques for coating of various objects and equipments and generates large amounts of wastewater arising from the various complex steps involved in the process. In fact, electroplating wastewater consists of different heavy metals and contaminants at concentrations well above the permitted levels and some of them, particularly chromium (Cr) and nickel (Ni), are toxic even at low concentrations besides being harmful to the human health as well as to the environment. According to the technical surveys, Cr concentration in electroplating wastewater ranges from ten to hundreds of $mg.lit^{-1}$ while the permissible limits for discharge of Ni and Cr containing streams are 0.2 and 0.05 $mg.lit^{-1}$, respectively [1]. Thus, long term and sustainable operation of electroplating industry requires necessary attentions toward proper treatment of wastewaters.

Ion exchange, adsorption, electrochemical processes, solvent extraction, complexation and precipitation are among the most widely practiced methods for the treatment of electroplating wastewater and removal of heavy metals [2-8]. Some of the disadvantage and limitations of these methods are needing addition of chemicals, production of sludge, difficulty in reusing extracted heavy metal and high costs among others [5, 6, 9, 10]. On the other hand, since their evolution, membrane separation processes have offered advantages such as low energy consumption, continuous operation, modular design, high efficiency, minimal labor requirements, selective removal of pollutants, low cost, physical separation of contaminants as well as easy operations and maintenance [11-21]. Accordingly, application of membranes for effective treatment of electroplating wastewater has attracted many researchers and membranologists.

Among the available membrane based technologies consisting of reverse osmosis (RO), electrodialysis (ED), nanofiltration (NF), ultrafiltration (UF), microfiltration (MF) and complexation-ultrafiltration (CUF), NF has been examined as the high potential candidate for removal and recovery of heavy metals and multivalent ions from various types of wastewaters [6, 10, 22-25]. In NF, pressure gradient is driving force of process and separation mechanism lies between UF and RO membranes. NF membranes typically operate at pressures ~0.5–2 MPa and can be used for molecular weight cut-offs (MWCO) in the range of 200–1000 $g.mole^{-1}$ [26-28]. NF membranes are often designed to possess electrostatic charge at the surface in order to provide better rejection performance in addition to the size selectivity characteristics of the

membrane. Accordingly, the principal mechanisms in NF separation are combinations of charge effects and size exclusions.

Material selection, membrane design, formulation, fabrication as well as process configurations and operational conditions play the key roles in the success of NF membranes for any treatment. Accordingly, several aspects have been investigated by researchers to enhance the performance of NF membranes for targeted applications in the field of wastewater treatment [27, 29].

Selection of appropriate materials having desired properties is the main factor in preparation of membranes. Different types of polymeric materials have been employed to fabricate asymmetric NF membranes including aromatic polyamides, polyphenylene sulfone, polysulfone, polyethersulfone, cellulose acetate and poly (vinylidene fluoride). Among diverse materials, polyacrylonitrile (PAN) has been extensively used for making membranes for variety of applications due to the special characteristics such as possessing hydrophilic group, high thermal and chemical stability, good resistance to most organic solvents and commercial availability [30-42]. PAN is soluble in the polar solvents such as N-methyl-2-pyrrolidone (NMP), Dimethyle acetamide (DMAc) and imethyle formamide (DMF) [30, 31, 33, 42]. Due to attractive properties, PAN has been used as membrane material either for fabrication of UF membrane or in the capacity of substrate for thin film composite NF and RO membrane [41]. Also, PAN is recognized as a preferred choice compared to other common polymers (e.g., polysulfone, polyethersulfone, etc) for its relatively low fouling tendency in liquid filtration processes [43]. Paul et al. [33] investigated the separation properties and surface morphology of PAN ultrafiltration membranes. Polymer concentration varied from 10% to 17.5% and led to flux reduction from 1900 to 250 lit.m^{-2}.hr. This was attributed to reduction of membrane porosity as the polymer concentration increased. Nouzaki et al. [30] investigated PAN ultrafiltration membrane using PAN 70,000 and PAN 400,000 for water treatment in operating pressures in the range of 0.5-1 bar. Reduction in permeability and increase in dextran rejection were observed with increasing polymer concentration. Due to the flux reduction with increasing PAN concentration, they used poly(vinylpyrrolidone) (PVP) in order to increase flux. In overall, PAN membranes demonstrated low susceptibility to chlorine attack and good resistance against cleaning agents [43].

In addition to material selection, improving the structure of membranes has been subject of various studies [44-48]. Different approaches such as bulk modification, blending and surface

treatment have been used for tuning the intrinsic properties of base polymer. Embedding of additives has also been considered as one of the efficient techniques for surface improvement in terms of hydrophilicity, roughness, surface charge and pore size. Many types of materials including hydrophilic polymers, amphiphilic polymers, and inorganic materials have been explored as additive. Poly (vinylpyrrolidone) (PVP) and polyethylene glycol (PEG) are among the most common hydrophilic additives used as a pore former to improve the permeate flux. PEG is a polymer with different chain lengths having low toxicity and good miscibility in water and other common solvents [3, 49]. PEG as a pore former imparts hydrophilicity due to having chains with highly hydrophilic nature and leads to formation of a porous structure with direct influence on the flux [26, 49-51]. Akbari et al. [26] utilized PEG with different molecular weights for preparation of polysulfone based membranes and their findings indicated that increasing the molecular weight of PEG from 200 to 600 Da in membrane preparation step led to increase in pore size and MWCO from 3.42 to 4 nm and from 6000 to 8000 Da, respectively. Saljoughi et al. [52] investigated the effect of changing PEG concentration on the membrane performance and morphology. Addition of PEG into the dope solution led to formation of macrovoids in sublayer and increasing of permeate flux and membrane final thickness.

On the other hand, several studies have been carried out on the possibility of improving the performance of membranes by incorporation of nanoparticles and inorganic additives [24, 28, 53-62]. For instance, Daraei et al.[24] studied the effects of embedding surface modified iron II and III oxide (PANI/Fe_3O_4) nanoparticles on the performance and morphology of polyethersulfone NF membranes for Cu (II) removal from water. They showed the membrane containing 0.1 wt.% PANI/Fe_3O_4 nanoparticles offered the highest Cu (II) ion removal efficiency while the pure water flux was very low due to the partial pore blockage caused by the particles. In another study, Gholami et al. [53] investigated lead removal from water by nanofiltration membranes prepared from polyvinyl chloride containing Fe_3O_4 nanoparticles. The modified membrane containing 0.1 wt.% Fe_3O_4 nanoparticles showed the highest lead rejection performance.

Among the various types of nanomaterials, titanium dioxide (TiO_2) exhibits photo-catalytic and super hydrophilicity properties that can influence antifouling characteristics and permeability simultaneously [54, 57]. The properties and performance of modified polysulfone NF membranes containing different size and loadings of TiO_2 nanoparticles was studied by

Vatanpour et al [57]. They reported that use of nanoparticles in membrane led to an increase in hydrophilicity and permeability. It also affected the pore radius and porosity of membrane. At high nanoparticles loading, the permeate flux of mixed matrix membrane decreased due to agglomeration of nanoparticle, especially at membrane skin layer. Despite the potential advantages of PAN itself, only limited studies are devoted to the applications of PAN for wastewater treatment and particularly for separation of heavy metals ions from electroplating waste streams.

The aim of the present study is to perform a systematic investigation on development of NF membranes from PAN by exploring the effects of prominent formulation, fabrication and operational parameters. In addition, the effects of addition of TiO_2 nanoparticles (as an inorganic additive) and PEG (as an organic additive) for tuning the structure, surface characteristics and separation efficiency of the developed membranes are being examined. The experiments and results are analyzed using appropriate statistical analysis as a useful tool with the objective of optimizing nickel and chromium rejection and water flux. To the best of our knowledge, and based on the detailed review, this is the first report on the exploitation of PAN as the selective material in fabrication of NF membranes for electroplating wastewater treatment.

2. Experimental

2.1. Materials

Poly (acrylonitrile) (MW=90,000 $g.gmol^{-1}$) in the form of white powders was purchased from Polyacryl Co., Isfahan, Iran. Dimethylformamide (DMF) and Poly(ethylene glycol) (PEG 4000) (CAS No.: 25322-68-3) were purchased from Merck (Germany) and used as the solvent for preparation of polymer solutions and as additive to the dope solutions, respectively. The chemical structures of PAN, DMF and PEG are shown in Fig. 1.

Titanium dioxide (TiO_2) nanoparticles (CAS No.: 13463-67-7) were purchased from US Research NanoMaterials and used as inorganic additive in the dope solutions. The properties of TiO_2 particles are provided in Table 1. Nickel and Chromium salts in the forms of $NiSO_4.6H_2O$ and $K_2Cr_2O_7$ (purity>99%) were supplied by Merck and used for preparation of synthetic aqueous solutions. Polyeseter based nonwovens (Hollytex #3329; basis weight: 96.5 $g.m^{-2}$, thickness: 0.135 mm, air permeability: 41 $L.m^{-2}.s^{-1}$) were purchased from Ahlstrom Corp. and used as substrate for casting of membranes.

2.2. Membrane fabrication

Flat sheet membranes were fabricated through phase inversion technique by preparing homogenous polymeric solution containing PAN, PEG, and TiO_2 in DMF according to the following procedures: Firstly, prescribed amounts of PAN powders were dried for at least 5 hours at 100°C in oven before being added to the solvent. For preparation of pure polymeric membranes, the powders were gradually added to the solvent while continuously stirring (500 rpm) and heating (60° C) until homogenous solutions obtained. For membranes containing PEG, both PAN and PEG were added together following the procedure used for pure polymer. However, for preparation of mixed matrix membranes, calculated amounts of nanoparticles were gradually added to the solvent followed by sonication for 10 min. Polymer powders were then added to the solution while stirring.

All the solutions were stored for overnight at ambient temperature to ensure no bubbles are trapped. Solutions were poured onto the nonwoven polyester substrates followed by leveling the surface (gap: 200 micron) at a constant speed using a semi-automated knife casting machine. The nascent films were immediately immersed into the coagulation bath containing tap water maintained at room temperature (25°C). All membranes were remained in water for at least 24 hrs to complete the coagulation process. Membranes were stored in cyclically refreshed water until performance tests. Based on the experimental design procedures, the concentration of PAN, PEG and TiO_2 varied in the range of 21-25 wt.%, 0-1.5 wt.% and 0-1 wt.%, respectively.

2.3. Characterizations

2.3.1. Morphological studies

Scanning electron microscopy (SEM) analysis was performed on a Philips SEM by exposing membrane surface and cross section to a beam of electrons at a certain accelerating voltage. Membranes were cut into small size and then submerged in liquid nitrogen before being broken. Membrane samples were gold-coated to enable electric conductivity [53, 63].

2.3.2. Water content & porosity measurements

The water content (WC) test is a measure of membrane hydrophilicity and can be calculated through Eq. 1 as follows:

$$WC\ (\%)=\frac{(Wwet-Wdry)}{Wdry}*100 \quad (1)$$

The procedure was carried out by submerging certain samples of dry membrane in water at 25°C for 24 hrs. Soaked samples were then removed and the surface waters were wiped off before weighing. Samples were then dried in oven at 50°C for 8 hrs and weighed again. This procedure was repeated at least five times to obtain reproducible results [24, 53].

Porosity (ε) is the volume fraction of interstitial spaces in membrane structure and can be calculated according to Eq. 2 [64]:

$$\varepsilon\ (\%)=\frac{(Wwet-Wdry)}{A.l.\rho}*100 \quad (2)$$

where ρ is water density (Kg.m^{-3}), l is membrane thickness (m) and A is membrane effective surface area (m^2).

Membrane mean pore radius (r_m) was determined using Guerout–Elford–Ferry equation using Eq. 3 [65]:

$$r_m=\sqrt{\frac{(2.9-1.75\varepsilon)\times 8\eta l Q}{\varepsilon A \Delta p}} \quad (3)$$

where, r_m is mean pore radius (m), η is water viscosity (at 25°C), l is membrane thickness (m), Q is the volumetric flow rate of the permeated water (m^3.h^{-1}), A is membrane effective surface area (m^2), ε is membrane porosity and ΔP is the testing pressure (10 bars).

2.3.3. Contact angle

The information arising from contact angle analysis can determine the degree of hydrophobicity or hydrophilicity of a membrane surface. This was performed using the sessile drop method with a goniometer (G10 KRUSS, Germany). A distilled water droplet was placed onto the membrane top surface and the contact angle between the water drop and the membranes was measured. In order to ensure reproducibility, measurements were carried out more than 10 times and at different spots.

2.4. Performance Evaluation

Performance evaluations were carried out using synthesized solutions based on a typical electroplating wastewater. Certain amounts of metal salts were dissolved in distilled water and solutions containing 50 mg.lit^{-1} $NiSO_4 \cdot 6H_2O$ and 50 mg.lit^{-1} $K_2Cr_2O_7$ were obtained.

Experiments were carried out on a cross-flow permeation set-up schematically presented in Fig. 2.

Effective surface area for each membrane was ~15 cm^2. In order to avoid possible membrane compaction during the experiments, each membrane was pressurized for 1 hr at 20 bar using water before conducting pure water flux and rejection tests. The actual runs were performed at 10 bar and 25±3°C. Both permeate and retentate streams were returned into the feed tank and recycled (except during sample collection) in order to maintain feed composition within the range until steady state conditions reached. After each run, the membrane cell and tube lines were fully rinsed with distilled water for 30 min at 5 bar to ensure no interference in subsequent runs.

The water flux (J_w) was calculated according to Eq. 4:

$$J_w = \frac{V}{A * \Delta t} \quad (4)$$

where V is the volume of permeated water from the membrane (L), A is the membrane effective surface area (m^2) and Δt is the duration of permeate collection (hr). Pure water flux was measured using distilled water at 25±3° C. A plot of pure water flux versus pressure gives a slope that is pure water permeability (L_P) and can be calculated using Eq. 5.

$$L_p = \frac{J_w}{\Delta P} \quad (5)$$

Rejection tests were carried out using synthetic salt solutions. Cr and Ni rejection were calculated using Eq. 6 [53]:

$$R = 1 - \frac{C_p}{C_f} \times 100 \quad (6)$$

where C_p and C_f are concentrations of Cr and Ni ions in permeate and feed, respectively. Concentrations of Ni and Cr in the feed and permeate were measured by an atomic absorption spectrophotometer (SHIMADZU, Japan)

2.5. Statistical analysis

RSM technique was employed using Design-Expert 6.0.2 software for optimization of the results [66-68]. The effects of independent variables including PAN, PEG and TiO_2 concentration at three levels on pure water flux and Cr and Ni rejection were investigated. The most general response surface method is the central composite design (CCD). 2^3 factorial designs with six axial points and six central points were selected. In order to obtain a good estimation of

experimental error, central points were repeated for six times. The trend of the system was fitted using a quadratic model according to Eq. 7:

$$y = \beta_0 + \sum_{i=1}^{n} \beta_i X_i + \sum_{i=1}^{n} \beta_{ij} X_i^2 + \sum_{i=1}^{n-1} \sum_{j=i+1}^{n} \beta_{ij} X_i X_j + \varepsilon \quad (7)$$

In this equation, y is the response, β_0 is a constant coefficient, X_i is non-coded variable, β_i is linear interaction coefficient, β_{ii} is the quadratic interaction coefficient, β_{ij} is the second order interaction coefficient, ε is the residual of each experiment. Table 2 provides a list of independent variables and coded levels. Also Table 3 provides the list of the samples and their corresponding independent variables and responses.

3.Results and discussion

3.1.Effect of polymer concentration on the morphology and performance of NF membranes

The SEM analysis was used to evaluate how the polymer concentration affects the membrane morphology (Fig. 3). A comparison between these images reveals that polymer content had significant impact on the cross section morphology. A low polymer concentration led to a more porous membrane with more finger-like macrovoids which extend from the top (sir side) to bottom (glass side) surfaces of the membrane. As reported in literature, an instantaneous demixing makes finger-like macrovoids whereas delayed demixing results in sponge-like structure. By increasing the polymer concentration from 21 wt % to 25 wt %, the finger-like macrovoids vanished and spongy-like structure expanded throughout of the membrane. Moreover, the area fraction of macrovoids in sub-layer became smaller, causing a decrement in final thickness of prepared membrane. Similar results were reported in case of other integrally asymmetric NF membranes [69, 70].

The variation of porosity and mean pore size of membranes with change in polymer concentration is provided in Table 4. By increasing the polymer concentration in dope solution from 21 wt.% to 25 wt.%, the mean pore size and porosity of fabricated membrane decreased from 10.15 nm to 7.99 nm and from 59.44% to 44.41%, respectively. The trend of variation of the mean pore size and porosity is matched with the trend of the pure water flux. At lower PAN concentration, the delayed demixing occurs which suppresses the formation of finger-like pores and reduces the porosity of membrane due to increased solution viscosity. Moreover, According

to Fig. 4 (a) and (b), the contact angle of the membranes increased from 43.3° to 59.98° whereas the water content decreased from 52.87 to 39.14 by increasing of PAN concentration from 21 wt.% to 25 wt.%, respectively. The results are in good agreement with previously reported findings [40, 51, 61]. As reported by Sotto et al. [56], higher polymer concentration affects the surface porosity and surface roughness and changes the contact angle based on Wenzel's model. Given that both membranes are made from PAN, the greater contact angle of the membrane fabricated using the casting solution with a more PAN content, can strongly be related to the decreased porosity of membrane surface.

The influence of polymer concentration on the pure water flux of the PAN membranes is shown in Fig. 5 (a). Results indicates that an increase in PAN content in casting solution from 21 wt% to 25 wt% corresponds to a decrease in pure water flux from 94.86 $Lit.m^2.h^{-1}$ to 41.35 $Lit.m^2.h^{-1}$, respectively. This can be described by the increase in dope solution viscosity with increasing PAN concentration, which hampers the penetration of non-solvent (water) into polymer film and reduces the diffusional exchange rate between solvent and non-solvent during solidification (phase inversion) process. Increased viscosity acts as a void-suppressing agent and changes the path of demixing process from instantaneous to demixing. It is reported in literature that the delayed demixing leads to sponge-like structures with lower porosity and permeability.

Increasing the polymer content in the casting solutions strongly altered the separation efficiency of prepared membranes for Ni and Cr rejections. According to Fig. 6, Ni and Cr rejection increased from 60.87% to 80.36% and from 56.36% to 78.64% upon increasing PAN concentration in the dope from 21 wt% and 25 wt%, respectively. Rejection of solute by NF membrane is governed with two mechanisms: (1) size exclusion and (2) electrostatic charge repulsion combined with Donnan effect. According to Table 4, higher polymer content decreases the pore size of membrane, resulting in improvement of solute rejection based on size exclusion mechanism. Moreover, PAN has negative surface charge in nature. Therefore, the separation mechanism of PAN-derived membranes is also influenced by electrostatic charge repulsion and Donnan effect.

3.2.Effect of PEG concentration on the morphology and performance of NF membranes

The effects of hydrophilic nature of PEG and its concentration in casting solution on the structure and separation efficiency of PAN-derived membrane were investigated. Based on literature survey [50], PEG may potentially augment the performance of the membranes through inducing hydrophilicity and optimizing both surface and bulk morphology. According to the experimental design, this examination carried out in the case of membranes containing 23 wt. % PAN and 0.5 wt. % TiO_2 dissolved in DMF. Fig. 7 shows the SEM cross section micrographs of membranes fabricated with different concentration of PEG. All prepared membranes illustrated in Fig. 7, display an integrally asymmetric structure including a dense skin layer and a porous sub-layer with finger-like macrovoids extended from top to bottom of membrane. It is clear that by increasing PEG concentration the selective layer thickness increased, the size and geometry of finger-like macrovoids changed and the uniformity of macrovoids improved. According to SEM analysis, PEG acts as pore forming agent during the formation of membrane structure. The addition of PEG in the dope solutions has two opposite effects. (1) As reported in literature [71], existence of PEG increases the viscosity of dope solution. It suppresses the formation of finger-like macrovoids after immersion in coagulation bath. Increased viscosity reduces the solvent (DMF) and non-solvent (water) exchange rate during solidification process. (2) PEG has hydrophilic properties. Addition of PEG decreases the thermodynamic stability of dope solution, which causes rapid instantaneous demixing and accelerates the formation of finger-like macrovoids during solidification process [71]. In current research, it seems that later effect is governed.

Porosity, mean pore size, membrane thickness, and area fraction of macrovoids were also obtained. According to the data in Table 5, porosity, mean pore size as well as the area fraction of macrovoids gradually increased by increasing the PEG concentration. In fact, addition of a low amount of PEG makes the dope solution thermodynamically instable. However, at high PEG loading, increased viscosity of dope solution results in kinetic hindrance during phase inversion process. In this study, low amounts of PEG were used and thermodynamic instability and consequently instantaneous demixing governed the phase inversion process [28]. Instantaneous demixing causes the formation of macrovoids in sub-layer and more porous structure at top - layers. Increasing the PEG content also increased the membrane thickness because the precipitation process is stopped more quickly, which is in good agreement with literature [26, 30]. According to Fig. 4, it was also found that the addition of PEG slightly altered the

hydrophilicity of the membrane surface owing to the intrinsic hydrophilic nature of the PEG and its transfer toward membrane surface during the membrane formation process, [59].

As shown in Fig. 5, addition of PEG from 0 wt% to 1.5 wt% enhanced the pure water flux from 65.40 lit.m^2.h^{-1} to 100.29 Lit.m^2.h^{-1}, respectively. It is clear that utilization of PEG as additive significantly enhanced the pure water flux. As expected, the pure water flux of the modified membranes was higher than that for the bare ones. In fact, the embedding of PEG into the polymer matrix enhances the wettability and porosity of the prepared membrane, which results in higher pure water flux. Since PEG is soluble additive in water, the major amount of PEG is extracted from the polymer film during the membrane formation process and only residuals remain within the membrane matrix. Thus, the main contribution of PEG to the membrane characteristics can be attributed to the pore formation and alteration of morphology than altering the wettability and surface characteristics [50].

the impacts of PEG content on the separation efficiency is illustrated in Fig. 6. It is obvious that the retention of Ni and Cr ions decreased by addition of higher content of PEG in the casting solutions. The Ni and Cr rejection decreased from 82.88% to 75.36 and from 79.42% to 73.51 in NF membranes prepared using dope solutions (23 wt.% PAN) containing 0 wt.% and 1.5 wt.% of PEG, respectively. Similar trends were found on the effects of PEG content on cellulose acetate membranes performance for rejection of dextran and HSA [52, 72]. The decrease in ion rejection with increasing PEG concentration may be due facilitated transfer rate of PEG and water (non-solvent) during precipitation process, resulting in larger pores on the membrane surface as also evidenced from mean pore size data in Table 5.

3.3. Effect of TiO_2 nanoparticle concentration on the morphology and performance of NF membranes

Several research works have considered the advantages of addition of nanoparticles on the membrane properties and performance. Nanoparticles are used to enhance antifouling properties, water transport, and physicochemical properties of membrane due to surface functional groups and hydrophilic properties of some nanoparticles, through improving interactions between nanomaterials/polymer matrix/solvents system. Fig. 8 shows the pure water flux of NF membranes prepared using different concentration of TiO_2 as inorganic additive. The pure water

flux improved form 84.28 $Lit.m^2.h^{-1}$ to 93.97 $Lit.m^2.h^{-1}$ upon increasing TiO_2 in the casting solution from 0 wt.% to 1 wt.%. The main factors contributing to the permeation flux of the membrane are surface pore size, porosity, skin layer thickness, and hydrophilicity. The porosity results display that the porosity of all prepared membranes improved by incorporation of nanoparticles. Entrapped nanoparticles in polymer matrix can alter the interaction between polymer chains and solvent (DMF) molecules, accelerated the exchange of solvent and non-solvent. Therefore, the porosity of nano-composite membrane could be higher than bare PAN membrane.

The contact angle results also exhibited in Fig. 4. As shown in Fig. 4 (c) and (d), by incorporating the TiO_2 nanoparticles into polymer matrix, contact angle of prepared membranes significantly decreased, ,. The significant change in contact angle can be related to hydrophilic nature of TiO_2 nanoparticles. The unmodified membrane had the lowest hydrophilicity. By increasing the TiO_2 nanoparticles concentration up to 1.5 wt. %, the contact angle continuously declined. The increased hydrophilicity and porosity improved the pure water flux through facilitating the penetration of nano-solvent molecules to the membrane medium and its diffusion within the membrane. Fig. 9 shows the cross section morphology of the membranes containing various amounts of TiO_2 nanoparticles. The skin layer and sub-layer have dense and spongy-like structures, respectively. The structure of membrane as well as geometry of macrovoids turned into a more uniform shape upon increasing the TiO_2 concentration. In fact, membrane containing more TiO_2 seems to have larger macrovoids than those with no or lesser TiO_2. The hydrophilicity of TiO_2 particles and their presence on the surface of the nascent film which can promote the intrusion of water during phase inversion [56, 73]. According to data in Table 5, initially, both mean pore size and area fraction of macrovoids increased and then decreased with increasing of TiO_2 concentration which may be due to the possible agglomeration of nanoparticles at high concentration (i.e., 1%) of TiO_2. The SEM images of the top surface of the membranes containing TiO_2 are shown in Fig. 10. According to these images and overall observations of the surface, nanoparticles were almost uniformly dispersed on the surface regardless of the presence of PEG (e.g., Fig. 10 (c) and (c')) or their absence (e.g., Fig. 10 (b) and (b')).

Considering the effect of nanoparticles on the performance of membranes are exhibited in Fig. 11. Data revealed that both Ni and Cr rejection were considerably increased upon incorporation of TiO_2 nanoparticles into the membrane matrix. Slight improvements in the rejections were

achieved upon addition of more TiO_2 into the membrane. According to Fig. 10, the addition of optimum amount of nanoparticles into dope solution accompanied with good dispersion can augment the solute rejection. The high loading of nanoparticles can produce the aggregates, In addition, the casting solution viscosity increases at the high loading of nanoparticles. Increased viscosity lead to slow demixing process and allow the nanoparticles to be aggregated near each other. At high loading, the nanoparticles tend to attract to each other by van der Waals forces and led to the agglomeration and reduction in the surface energy [10, 51].

3.4. Statistical analysis

Nowadays, membrane manufactures try to improve the morphology of membranes and to optimize the process conditions [74-77]. In conventional experimentation methods, the effects of each variable are investigated while other parameters are remained constant. This procedure often involves many experimental runs, ignores interaction effects between the parameters, is time consuming and potentially leads to low efficiency in the optimization process. Statistical analysis is a useful tool and can overcome these limitations by employing an appropriate statistical method. Response surface methodology (RSM) provides a statistical design of experiments through which all factors change together over a set of experimental runs. In fact, RSM is regarded as a combination of mathematical and statistical techniques for improving, developing and optimizing processes and can be utilized for evaluation of the relative significance of the independent process factors, particularly when complex interactions exist. By using RSM, response surface plots provide information about relationship between the factors and responses. The design of experiments (DoE) and RSM have been successfully employed in various technical and scientific fields such as applied physics and chemistry, biological, biochemistry, environmental protection, chemical engineering as well as for membrane process systems [78-80]. Accordingly, this technique was used for analysis of the findings in this study.

The quadratic polynomial response surface model (Eq. 7) was appropriate for all of the responses. Evaluation of each response was done as a function of linear, quadratic and interaction terms of independent variable including PAN, PEG and TiO_2 concentration. In order to examine the statistical significance of the terms and model fitting, ANOVA and regression

analysis was used. Table 6 shows the regression coefficients for the quadratic polynomial models and corresponding coefficient of determination (R^2) for each response.

In addition, the coefficient of variation (CV) and adj-R^2 was checked for adequacy of models. The R^2 values were 0.9835, 0.9749, and 0.9929 for Ni rejection, Cr rejection and pure water flux respectively. The higher R^2 shows the model desirability to demonstrate the relationship between variables. Since R^2 is greater than 0.8, models were appropriate to present the trends. However, when the value of R^2 is closer to one, the models fit the actual data. The lower value for R^2 indicates that model is not suitable for illustrating the relation between variables. It should be noted that R^2 will always increase upon addition of more variables to the model, regardless of statistically significance of the variable. Therefore, a large R^2 does not always guarantee the appropriateness of the model. For this reason, it is more appropriate to utilize an adjusted-R^2 of over 90% to evaluate the model adequacy. A significant lack of fit shows that the model is not successful to display the data in the experimental domain at which points were not included in the regression [81]. The lack of fit of all variables was not significant ($p>0.05$) indicating that all of models correctly predicted the related responses. CV demonstrates the extent to which the data has dispersed. Generally, CV should not be greater than 10%. A large CV represent that mean value variation is high and does not develop an adequate and satisfactory response model [81]. According to the data in Table 6, the results indicated that the CV was less than 10% for all the responses, it show a better accuracy and reliability of the conducted experiments. In fact, the quadratic model was able to predict the responses with good estimation.

The *p*-values can be employed as a factor to evaluate the importance of every coefficient. This factor is crucial to investigate the pattern of mutual interactions between the experiment variables. The smaller value of *p* implies that the studied coefficient is more important. Thus, model terms are important when *p*-values are less than 0.05 [81]. From the model of Ni rejection and according to data in Table 6, linear effect of PAN, PEG and TiO_2 concentration, the quadratic effect of PAN and TiO_2 were significant ($p<0.01$). Based on the sum of square, the importance of independent variables on Ni rejection ranked in the following order: PAN concentration > TiO_2 concentration> PEG concentration. In addition, the results indicate that the largest effect firstly related to linear and quadratic term of PAN concentration then to TiO_2 concentration.

The result of Cr rejection in Table 6 show that the linear effect of PAN, PEG and TiO_2 concentration and quadratic effect of PAN and TiO_2 were significant ($p<0.01$) and indicate mutual interaction between variables has not significant effect on Cr rejection. Based on the sum of square, the importance of independent variables on Cr rejection is similar to Ni rejection. The given results in Table 6 show that linear extraction PAN, PEG and TiO_2 concentration had the significant effects on pure water flux ($p < 0.0001$, $p < 0.01$). Quadratic effects of PAN and PEG concentration were significant at less than 0.01. The results also illustrate that among the interactions, PAN and PEG concentration had significant effects on pure water flux ($p < 0.01$). Fig. 12 shows that the quadratic model is in appropriate agreement with the experimental results. In this figure, each experimental value is compared to the corresponding model predicted value. The results indicate that the models used in this research can predict the best membrane formulation.

3.5.Optimization

The objective of optimization in response surface is to find a desirable situation in the design space. This could be a minimum, a maximum, or an area where the response is stable over a range of factors [82]. The optimum condition for PAN, PEG and TiO_2 concentration was determined to obtain maximum Nickel and Chromium rejection and pure water flux. This optimum condition is provided in Table 7 showing the best value for Nickel rejection (87.093 %), chromium rejection (83.271 %) and pure water flux (71.801 $Lit.m^{-2}.h^{-1}$). Fig. 13 (a) and (b) present the overlaying plots for the three responses that evaluated as a PAN, PEG and TiO_2 concentration. These plots show the best combination factors. A small shaded area of the three responses is determined as the optimum area that displays a larger value for Ni and Cr rejection and pure water flux. Fig. 14 also shows the pure water permeability for the optimized membrane. The pure water flux rises linearly with increase of applied pressure. According to Eq. 5, permeability of the optimized membrane is 14.598 that is a typical value in the range of nanofiltration membranes permeability. Table 8 provides the performance data for several commercial and non-commercial NF membranes [81, 83-86]. It is clear that the water flux for the optimized membrane fabricated in present study stands better than the other listed membranes. This result can be due to desired porosity and thickness of prepared membranes. The Ni and Cr ions rejection of prepared membranes seems to be satisfactory considering the

operating pressure of present study compared to the testing pressure for the rivals. Also, the Ni rejection was higher than Cr rejection.

4. Conclusions

The effects of PAN, PEG and TiO_2 nanoparticles concentration on membranes characteristics, such as morphology, wettability (contact angle), pure water flux and nickel and chromium rejection, were investigated. In order to analyze the interaction between the independent factors, Response Surface Methodology (RSM) was utilized. The results showed that the effects of PAN, PEG and TiO_2 concentration were statistically significant. Among the investigation parameters, PAN concentration had the greatest effect on membrane performance and morphology. Increase in PAN concentrations resulted in membranes with less porosity and mean pore size, having limited finger-like voids in the internal microstructure and a denser layer on top. At the same time, pure water flux decreased and Ni and Cr rejection increased. Increase in PAN concentration also led to increase in membrane contact angle. Ni and Cr rejection decreased when PEG concentration enhanced, whereas pure water flux, porosity and mean pore size were increased. In addition, an increase in PEG concentration led to an increase of the macro-void area. The addition of TiO_2 nanoparticles and rise of its concentration led to increasing pure water flux, Ni and Cr rejection. Optimum formulation was found to be PAN: 23.93 wt. %, PEG: 0.41wt. % and TiO_2: 0.82 wt. %. At this optimum point, Ni and Cr rejections as well as pure water flux were 87.093 (%), 83.271 (%) and 71.801 ($Lit.m^{-2}.h^{-1}$), respectively which are in good agreement with validation experiment. This investigation could help electroplating and similar industries to treat wastewater for the aim of reusing metals and treated water.

Acknowledgements

Authors would like to thank Iran Nanotechnology Initiative Council for the supports provided in the course of this project.

References

[1] S.S. Hosseini, E. Bringas, N.R. Tan, I. Ortiz, M. Ghahramani, M.A. Alaei Shahmirzadi, Recent progress in development of high performance polymeric membranes and materials for metal

plating wastewater treatment: A review, Journal of Water Process Engineering, 9 (2016) 78-110.
[2] A.G. Boricha, Z. Murthy, Preparation, characterization and performance of nanofiltration membranes for the treatment of electroplating industry effluent, Separation and purification technology, 65 (2009) 282-289.
[3] J.W. Wang, Y.M. Kuo, Preparation of fructose-mediated (polyethylene glycol/chitosan) membrane and adsorption of heavy metal ions, Journal of applied polymer science, 105 (2007) 1480-1489.
[4] N. Adhoum, L. Monser, N. Bellakhal, J.-E. Belgaied, Treatment of electroplating wastewater containing Cu 2+, Zn 2+ and Cr (VI) by electrocoagulation, Journal of Hazardous Materials, 112 (2004) 207-213.
[5] E. Alvarez-Ayuso, A. Garcia-Sanchez, X. Querol, Adsorption of Cr (VI) from synthetic solutions and electroplating wastewaters on amorphous aluminium oxide, Journal of Hazardous Materials, 142 (2007) 191-198.
[6] S.A. Cavaco, S. Fernandes, M.M. Quina, L.M. Ferreira, Removal of chromium from electroplating industry effluents by ion exchange resins, Journal of Hazardous Materials, 144 (2007) 634-638.
[7] A.I. Alonso, B. Galan, A. Irabien, I. Ortiz, Separation of Cr (VI) with Aliquat 336: Chemical Equilibrium Modeling, Separation Science and Technology, 32 (1997) 1543-1555.
[8] B. Galan, A.M. Urtiaga, A.I. Alonso, J.A. Irabien, M.I. Ortiz, Extraction of Anions with Aliquat 336: Chemical Equilibrium Modeling, Industrial & Engineering Chemistry Research, 33 (1994) 1765-1770.
[9] I. Youri, P. Harrington, G. Stevens, Long-term performance of hollow fibre membrane solvent extraction modules used for Cr (VI) recovery from electroplating rinse water, Solvent Extraction and Ion Exchange, 18 (2000) 933-951.
[10] K.-H. Ahn, K.-G. Song, H.-Y. Cha, I.-T. Yeom, Removal of ions in nickel electroplating rinse water using low-pressure nanofiltration, Desalination, 122 (1999) 77-84.
[11] Y. Xiao, B.T. Low, S.S. Hosseini, T.S. Chung, D.R. Paul, The strategies of molecular architecture and modification of polyimide-based membranes for CO2 removal from natural gas—A review, Progress in Polymer Science, 34 (2009) 561-580.
[12] S.S. Hosseini, S.M. Roodashti, P.K. Kundu, N.R. Tan, Transport Properties of Asymmetric Hollow Fiber Membrane Permeators for Practical Applications: Mathematical Modeling For Binary Gas Mixtures Canadian journal of chemical engineering, 93 (2015) 1275-1287.
[13] S. Najari, S.S. Hosseini, M. Omidkhah, N.R. Tan, Phenomenological modeling and analysis of gas transport in polyimide membranes for propylene/propane separation, RSC Advances, 5 (2015) 47199-47215.
[14] S.S. Hosseini, S. Najari, P.K. Kundu, N.R. Tan, S.M. Roodashti, Simulation and sensitivity analysis of transport in asymmetric hollow fiber membrane permeators for air separation, RSC Advances, 5 (2015) 86359-86370.
[15] M.A. Alaei Shahmirzadi, S.S. Hosseini, G. Ruan, N.R. Tan, Tailoring PES nanofiltration membranes through systematic investigations of prominent design, fabrication and operational parameters, RSC Advances, 5 (2015) 49080-49097.

[16] S.S. Hosseini, J.A. Dehkordi, P.K. Kundu, Gas permeation and separation in asymmetric hollow fiber membrane permeators: Mathematical modeling, sensitivity analysis and optimization, Korean Journal of Chemical Engineering, (2016) 1-17.
[17] M. Tamaddondar, H. Pahlavanzadeh, S. Saeid Hosseini, G. Ruan, N.R. Tan, Self-assembled polyelectrolyte surfactant nanocomposite membranes for pervaporation separation of MeOH/MTBE, Journal of Membrane Science, 472 (2014) 91-101.
[18] M.A. Alaei Shahmirzadi, S.S. Hosseini, N.R. Tan, Enhancing Removal and Recovery of Magnesium from Aqueous Solutions Through Specialized Modification of Zeolite and Bentonite and Process Optimization, Korean Journal of Chemical Engineering, In Press (2016).
[19] S.S. Hosseini, S. Najari, Polymeric Membranes for Gas and Vapor Separations, in: P.M. Visakh, N. Olga (Eds.) Nanostructured Polymer Membranes, Applications, Wiley, 2016.
[20] J.A. Dehkordi, S.S. Hosseini, P.K. Kundu, N.R. Tan, Mathematical Modeling of Natural Gas Separation Using Hollow Fiber Membrane Modules by Application of Finite Element Method through Statistical Analysis, Chemical Product and Process Modeling, 11 (2016) 11-15.
[21] S.S. Hosseini, J.A. Dehkordi, P.K. Kundu, Mathematical Modeling and Investigation on the Temperature and Pressure Dependency of Permeation and Membrane Separation Performance for Natural gas Treatment, Chemical Product and Process Modeling, 11 (2016) 7-10.
[22] W. Zuo, G. Zhang, Q. Meng, H. Zhang, Characteristics and application of multiple membrane process in plating wastewater reutilization, Desalination, 222 (2008) 187-196.
[23] C. Xijun, C. Guohua, Y. Po-Lock, M. Yongli, Pilot scale membrane separation of electroplating waste water by reverse osmosis, Journal of Membrane Science, 123 (1997) 235-242.
[24] P. Daraei , S.S. Madaeni, N. Ghaemi, E. Salehi , M. Khadivi, R. Moradian, B. Astinchap, Novel polyethersulfonenanocompositemembranepreparedbyPANI/Fe3O4 nanoparticleswithenhancedperformanceforCu(II)removalfromwater, Journal of Membrane Science, (2012) 250-259.
[25] L.Y. Ng, A.W. Mohammad, C.P. Leo, N. Hilal, Polymeric membranes incorporated with metal/metal oxide nanoparticles: a comprehensive review, Desalination, 308 (2013) 15-33.
[26] A. Akbari, M. Homayoonfal, Fabrication of Nanofiltration Membrane from Polysulfone Ultrafiltration Membrane Via Photo olymerization, International Journal of Nanoscience and Nanotechnology, 5 (2009) 43-52.
[27] B. Al-Rashdi, D. Johnson, N. Hilal, Removal of heavy metal ions by nanofiltration, Desalination, 315 (2013) 2-17.
[28] S.Y. Lee, H.J. Kim, R. Patel, S.J. Im, J.H. Kim, B.R. Min, Polyamide thin-film nanofiltration membranes containing TiO2 nanoparticles, Desalination, (2008) 48-56.
[29] Y. Sato, M. Kang, T. Kamei, Y. Magara, Performance of nanofiltration for arsenic removal, Water Research, 36 (2002) 3371-3377.
[30] K. Nouzaki, M. Nagata, J. Arai, Y. Idemoto, N. Koura, H. Yanagishita, H. Negishi, D. Kitamoto, T. Ikegami, K. Haraya, Preparation of polyacrylonitrile ultrafiltration membranes for wastewater treatment, Desalination, 144 (2002) 53-59.
[31] Z.-G. Wang, L.-S. Wan, Z.-K. Xu, Surface engineerings of polyacrylonitrile-based asymmetric membranes towards biomedical applications: An overview, Journal of Membrane Science, 304 (2007) 8–23.

[32] E. Shekarian, E. Saljoughi, A. Naderi, Polyacrylonitrile (PAN)/IGEPAL blend asymmetric membranes: preparation, morphology, and performance, Journal of Polymer Research, 20 (2013) 1-9.
[33] D. Paul, H. Kamusewitz, H.G. Hicke, H. Buschatz, Separation properties and surface morphology of polyacrylonitrile membranes, Acta polymerica, 43 (1992) 353-355.
[34] J. Wang, Z. Yue, J.S. Ince, J. Economy, Preparation of nanofiltration membranes from polyacrylonitrile ultrafiltration membranes, Journal of membrane science, 286 (2006) 333-341.
[35] K. Wong, B. Liu, S. McCalla, B. Chu, B. Hsiao, Analysis of PAN and PEGDA Coated Membranes for Filtering Water with Reduced Fouling and Increased Heavy Metal Adsorption.
[36] Y. Xiuli, C. Hongbin, W. Xiu, Y. Yongxin, Morphology and properties of hollow-fiber membrane made by PAN mixing with small amount of PVDF, Journal of membrane science, 146 (1998) 179-184.
[37] J. Xu, X. Feng, P. Chen, C. Gao, Development of an antibacterial copper (II)-chelated polyacrylonitrile ultrafiltration membrane, Journal of Membrane Science, 413 (2012) 62-69.
[38] S. Yang, Z. Liu, Preparation and characterization of polyacrylonitrile ultrafiltration membranes, Journal of membrane science, 222 (2003) 87-98.
[39] Z. Yongfeng, W. Yu, X. Zhenliang, L. Fengkai, X. Zheng, J. Mei, Study on the treatment of polyacrylonitrile wastewater with nanofiltration [J], Industrial Water Treatment, 10 (2004) 004.
[40] S. Asadi, E. Shekarian, A. Tarighaleslami, Preparation and characterization of nano-porous Polyacrylonitrile (PAN) membranes with hydrophilic surface, International Journal of Nano Dimension, 6 (2015) 217.
[41] C. Feng, J. Xu, M. Li, Y. Tang, C. Gao, Studies on a novel nanofiltration membrane prepared by cross-linking of polyethyleneimine on polyacrylonitrile substrate, Journal of Membrane Science, 451 (2014) 103-110.
[42] I.-C. Kim, H.-G. Yun, K.-H. Lee, Preparation of asymmetric polyacrylonitrile membrane with small pore size by phase inversion and post-treatment process, Journal of Membrane Science, 199 (2002) 75-84.
[43] B. Jung, J.K. Yoon, B. Kim, H.-W. Rhee, Effect of molecular weight of polymeric additives on formation, permeation properties and hypochlorite treatment of asymmetric polyacrylonitrile membranes, Journal of membrane science, 243 (2004) 45-57.
[44] C. Xie, L. Zhang, Y. Liu, Q. Lv, G. Ruan, S.S. Hosseini, A direct contact type ice generator for seawater freezing desalination using LNG cold energy, Desalination.
[45] S.S. Hosseini, M.M. Teoh, T.S. Chung, Hydrogen separation and purification in membranes of miscible polymer blends with interpenetration networks, Polymer, 49 (2008) 1594-1603.
[46] M.A. Alaei Shahmirzadi, S.S. Hosseini, Environmental aspects of brine management in seawater desalination, IRAN-WATER RESOURCES RESEARCH, 10 (2015) 104-112.
[47] A. Soleimany, S.S. Hosseini, F. Gallucci, Recent Progress in Developments of Membrane Materials and Modification Techniques for High Performance Helium Separation and Recovery: A Review, Chemical Engineering & Processing: Process Intensification, (2017).
[48] A.R. Greenberg, E. Kujundzic, B. Krantz William, A. Yeo, S.S. Hosseini, Determination of pore size in porous materials by evaporative mass loss, in, US Patent 20130042670, 2011.
[49] Z.-L. Xu, T.-S. Chung, K.-C. Loh, B.C. Lim, Polymeric asymmetric membranes made from polyetherimide/polybenzimidazole/poly (ethylene glycol)(PEI/PBI/PEG) for oil–surfactant–water separation, Journal of membrane science, 158 (1999) 41-53.

[50] M. Homayoonfal, A. Akbari, M.R. Mehrnia, Preparation of polysulfone nanofiltration membranes by UV-assisted grafting polymerization for water softening, Desalination, 263 (2010) 217–225.
[51] A. Morao, I. Escobar, M. Pessoa de Amorim, A. Lopes, I. Goncalves, Postsynthesis modification of a cellulose acetate ultrafiltration membrane for applications in water and wastewater treatment, Environmental progress, 24 (2005) 367-382.
[52] E. Saljoughi, M. Amirilargani, T. Mohammadi, Effect of PEG additive and coagulation bath temperature on the morphology, permeability and thermal/chemical stability of asymmetric CA membranes, Desalination, 262 (2010) 72-78.
[53] A. Gholami, A. Moghadassi, S. Hosseini, S. Shabani, F. Gholami, Preparation and characterization of polyvinyl chloride based nanocomposite nanofiltration-membrane modified by iron oxide nanoparticles for lead removal from water, Journal of Industrial and Engineering Chemistry, 20 (2014) 1517-1522.
[54] Y. Mansourpanah, S. Madaeni, A. Rahimpour, A. Farhadian, A. Taheri, Formation of appropriate sites on nanofiltration membrane surface for binding TiO< sub> 2</sub> photo-catalyst: Performance, characterization and fouling-resistant capability, Journal of Membrane Science, 330 (2009) 297-306.
[55] I. Soroko, A. Livingston, Impact of TiO 2 nanoparticles on morphology and performance of crosslinked polyimide organic solvent nanofiltration (OSN) membranes, Journal of Membrane Science, 343 (2009) 189-198.
[56] A. Sotto, A. Boromand, S. Balta, J. Kim, B. Van der Bruggen, Doping of polyethersulfone nanofiltration membranes: antifouling effect observed at ultralow concentrations of TiO 2 nanoparticles, Journal of Materials Chemistry, 21 (2011) 10311-10320.
[57] V. Vatanpour, S.S. Madaeni, A.R. Khataee, E. Salehi, S. Zinadini, H.A. Monfared, TiO 2 embedded mixed matrix PES nanocomposite membranes: influence of different sizes and types of nanoparticles on antifouling and performance, Desalination, 292 (2012) 19-29.
[58] Y. Yang, H. Zhang, P. Wang, Q. Zheng, J. Li, The influence of nano-sized TiO< sub> 2</sub> fillers on the morphologies and properties of PSF UF membrane, Journal of Membrane Science, 288 (2007) 231-238.
[59] Y. Yuan, T.R. Lee, Contact angle and wetting properties, in: Surface science techniques, Springer, 2013, pp. 3-34.
[60] J. Kim, B. Van der Bruggen, The use of nanoparticles in polymeric and ceramic membrane structures: review of manufacturing procedures and performance improvement for water treatment, Environmental Pollution, 158 (2010) 2335-2349.
[61] S.S. Hosseini, Y. Li, T.-S. Chung, Y. Liu, Enhanced gas separation performance of nanocomposite membranes using MgO nanoparticles, Journal of Membrane Science, 302 (2007) 207-217.
[62] S.S. Hosseini, Membranes and Materials for Separation and Purification of Hydrogen and Natural Gas, in: Department of Chemical and Biomolecular Engineering, National University of Singapore, 2009.
[63] O. Agboola, J. Maree, R. Mbaya, Characterization and performance of nanofiltration membranes, Environmental chemistry letters, 12 (2014) 241-255.
[64] B. Chakrabarty, A. Ghoshal, M. Purkait, Effect of molecular weight of PEG on membrane morphology and transport properties, Journal of Membrane Science, 309 (2008) 209-221.

[65] C. Liao, J. Zhao, P. Yu, H. Tong, Y. Luo, Synthesis and characterization of low content of different SiO 2 materials composite poly (vinylidene fluoride) ultrafiltration membranes, Desalination, 285 (2012) 117-122.
[66] V. Pirouzfar, S.S. Hosseini, M.R. Omidkhah, A.Z. Moghaddam, Modeling and optimization of gas transport characteristics of carbon molecular sieve membranes through statistical analysis, Polymer Engineering & Science, (2013) n/a-n/a.
[67] S.S. Hosseini, M.R. Omidkhah, A. Zarringhalam Moghaddam, V. Pirouzfar, W.B. Krantz, N.R. Tan, Enhancing the properties and gas separation performance of PBI–polyimides blend carbon molecular sieve membranes via optimization of the pyrolysis process, Separation and Purification Technology, 122 (2014) 278-289.
[68] V. Pirouzfar, A.Z. Moghaddam, M.R. Omidkhah, S.S. Hosseini, Investigating the effect of dianhydride type and pyrolysis condition on the gas separation performance of membranes derived from blended polyimides through statistical analysis, Journal of Industrial and Engineering Chemistry, 20 (2014) 1061-1070.
[69] S. Hamzah, N.a. Ali, M.M. Ariffin, A. Ali, A.W. Mohammad, High performance of polysulfone ultrafiltration membrane, ARPN Journal of Engineering and Applied Sciences, 9 (2014) 2543-2550.
[70] S. Balta, M. Bodor, L. Benea, INFLUENCE OF POLYMER CONCENTRATION ON THE PERMEATION PROPERTIES OF NANOFILTRATION MEMBRANES, Tehnomus J., 18 (2011) 227-232.
[71] E. Saljoughi, M. Sadrzadeh, T. Mohammadi, Effect of preparation variables on morphology and pure water permeation flux through asymmetric cellulose acetate membranes, Journal of Membrane Science, 326 (2009) 627-634.
[72] W.-L. Chou, D.-G. Yu, M.-C. Yang, C.-H. Jou, Effect of molecular weight and concentration of PEG additives on morphology and permeation performance of cellulose acetate hollow fibers, Separation and purification technology, 57 (2007) 209-219.
[73] L.Y. Ng, C.P. Leo, A.W. Mohammad, Optimizing the incorporation of silica nanoparticles in polysulfone/poly (vinyl alcohol) membranes with response surface methodology, Journal of Applied Polymer Science, 121 (2011) 1804-1814.
[74] S.S. Hosseini, T.S. Chung, Carbon membranes from blends of PBI and polyimides for N2/CH4 and CO2/CH4 separation and hydrogen purification, Journal of Membrane Science, 328 (2009) 174-185.
[75] S.S. Hosseini, N. Peng, T.S. Chung, Gas separation membranes developed through integration of polymer blending and dual-layer hollow fiber spinning process for hydrogen and natural gas enrichments, Journal of Membrane Science, 349 (2010) 156-166.
[76] S.Ü. Çelik, A. Bozkurt, S.S. Hosseini, Alternatives toward proton conductive anhydrous membranes for fuel cells: Heterocyclic protogenic solvents comprising polymer electrolytes, Progress in Polymer Science, 37 (2012) 1265-1291.
[77] W.B. Krantz, A.R. Greenberg, E. Kujundzic, A. Yeo, S.S. Hosseini, Evapoporometry: A novel technique for determining the pore-size distribution of membranes, Journal of Membrane Science, 438 (2013) 153-166.
[78] S. Madaeni, N. Arast, F. Rahimpour, Y. Arast, Fabrication optimization of acrylonitrile butadiene styrene (ABS)/polyvinylpyrrolidone (PVP) nanofiltration membrane using response surface methodology, Desalination, 280 (2011) 305-312.

[79] J. Landaburu-Aguirre, E. Pongrácz, P. Perämäki, R.L. Keiski, Micellar-enhanced ultrafiltration for the removal of cadmium and zinc: use of response surface methodology to improve understanding of process performance and optimisation, Journal of hazardous materials, 180 (2010) 524-534.
[80] M. Khayet, M. Seman, N. Hilal, Response surface modeling and optimization of composite nanofiltration modified membranes, Journal of Membrane Science, 349 (2010) 113-122.
[81] J. Gao, S.-P. Sun, W.-P. Zhu, T.-S. Chung, Chelating polymer modified P84 nanofiltration (NF) hollow fiber membranes for high efficient heavy metal removal, Water Research, 63 (2014) 252-261.
[82] J. Mehrabani, M. Noaparast, S. Mousavi, R. Dehghan, A. Ghorbani, Process optimization and modelling of sphalerite flotation from a low-grade Zn-Pb ore using response surface methodology, Separation and Purification Technology, 72 (2010) 242-249.
[83] G. Basaran, D. Kavak, N. Dizge, Y. Asci, M. Solener, B. Ozbey, Comparative study of the removal of nickel(II) and chromium(VI) heavy metals from metal plating wastewater by two nanofiltration membranes, Desalination and Water Treatment, 57 (2016) 21870-21880.
[84] K. Linde, A.-S. Jönsson, Nanofiltration of salt solutions and landfill leachate, Desalination, 103 (1995) 223-232.
[85] X. Wei, X. Kong, S. Wang, H. Xiang, J. Wang, J. Chen, Removal of Heavy Metals from Electroplating Wastewater by Thin-Film Composite Nanofiltration Hollow-Fiber Membranes, Industrial & Engineering Chemistry Research, 52 (2013) 17583-17590.
[86] L.B. Chaudhari, Z.V.P. Murthy, Treatment of landfill leachates by nanofiltration, Journal of Environmental Management, 91 (2010) 1209-1217.

List of Figures:

(c&c') PEG: 0.75 wt.% TiO_2: 0.5 wt.% (conditions: PAN Conc.: 23 wt.%, solvent: DMF, coagulating agent: water, coagulation bath temperature: 25 °C, casting knife gap: 200 µm).

Fig. 11. Response surface for the effect of PEG and TiO_2 concentrations on Ni rejection (a) 3D surface (b) Contour and Cr rejection (c) 3D surface (d) Contour. (PAN conc.:23%)

Fig. 12. Comparison between experimental (actual) and predicted value for (a) Ni rejection, (b) Cr rejection and (c) pure water flux.

Fig. 13. The optimum region by overlaying plot of the three responses evaluated as a function of PAN, PEG and TiO_2 concentration (%) (a) at constant TiO_2=0.5% (b) at constant PAN=23%.

Fig. 14. The effect of feed pressure on pure water flux for optimized membrane
(PAN: 23.91%, PEG: 0.41%, TiO_2: 0.82%).

List of Tables

Table 1.The properties of TiO_2 nanoparticles used in this study.

Table 2. List of independent variables and their levels.

Table 3. The list of the samples and their corresponding variables and responses derived based on the experimental design.

Table 4. Effect of PAN concentration on porosity and mean pore size of the membranes.

Table 5. Effect of PEG and TiO_2 concentration on the characteristics of NF membranes.

Table 6. ANOVA regression coefficients for the quadratic polynomial models and corresponding coefficient of determination for each response.

Table 7. Predicted optimum condition for removal of Ni and Cr from wastewater

Table 8. Performance data for several commercial and non-commercial NF membranes

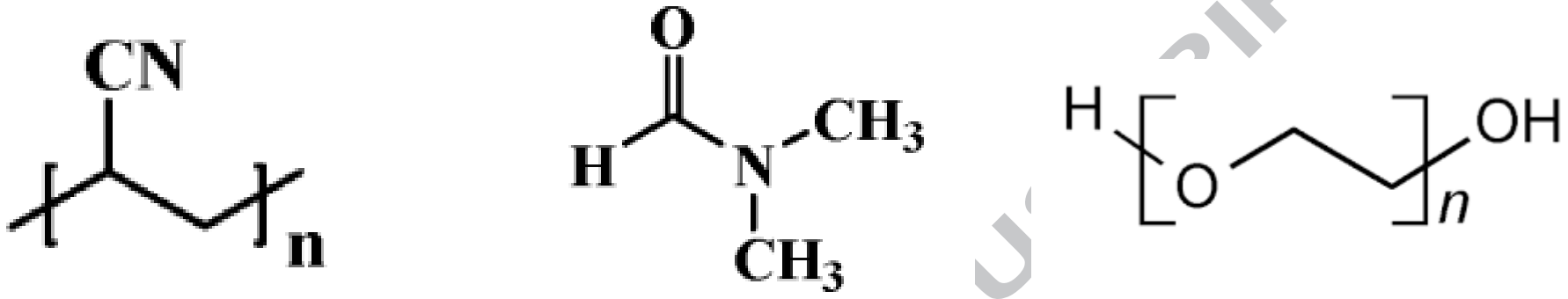

(a) (b) (c)

Fig. 1. Chemical structures of (a) PAN (b) DMF (c) PEG

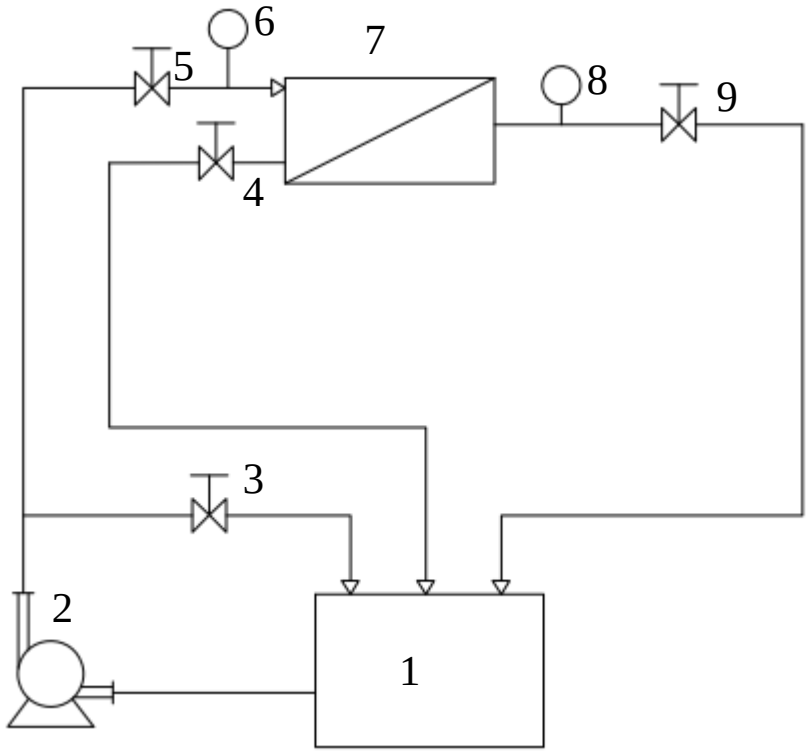

Fig. 2. Schematic of NF set-up (1- Feed tank, 2- Pump, 3- Bypass valve, 4- Back pressure regulator, 5-Feed valve, 6-Pressure gauge, 7- Membrane module, 8-Pressure gauge, 9- Permeate valve).

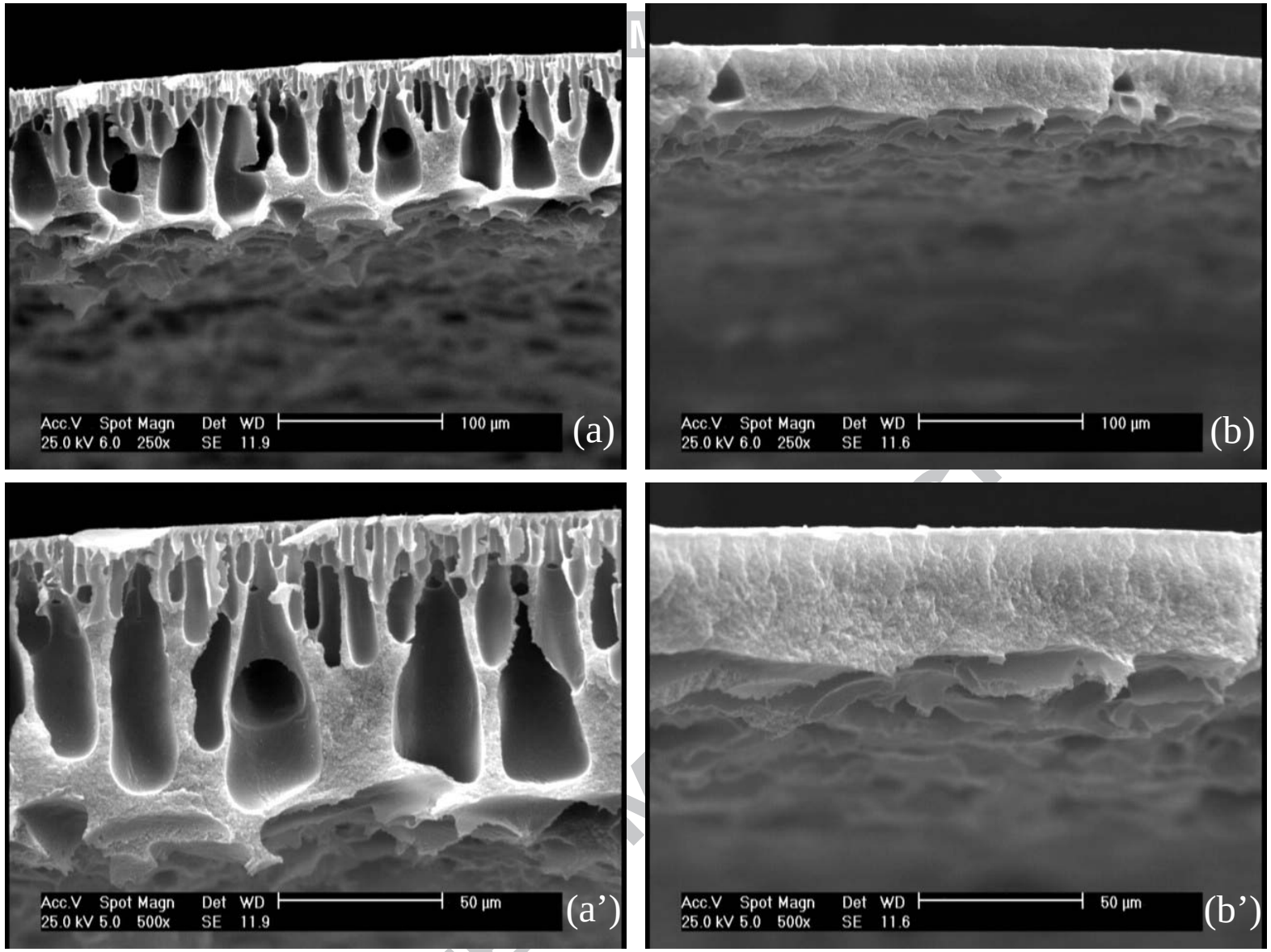

Fig. 3. The effect of PAN concentration in dope on the morphology of NF membranes (a) cross section PAN: 21 wt.% (a') skin layer PAN: 21 wt.% (b) cross section PAN: 25 wt.% (b') skin layer PAN: 25 wt.% (conditions: solvent: DMF, coagulating agent: water, coagulation bath temperature: 25 ˚C, casting knife gap: 200 µm).

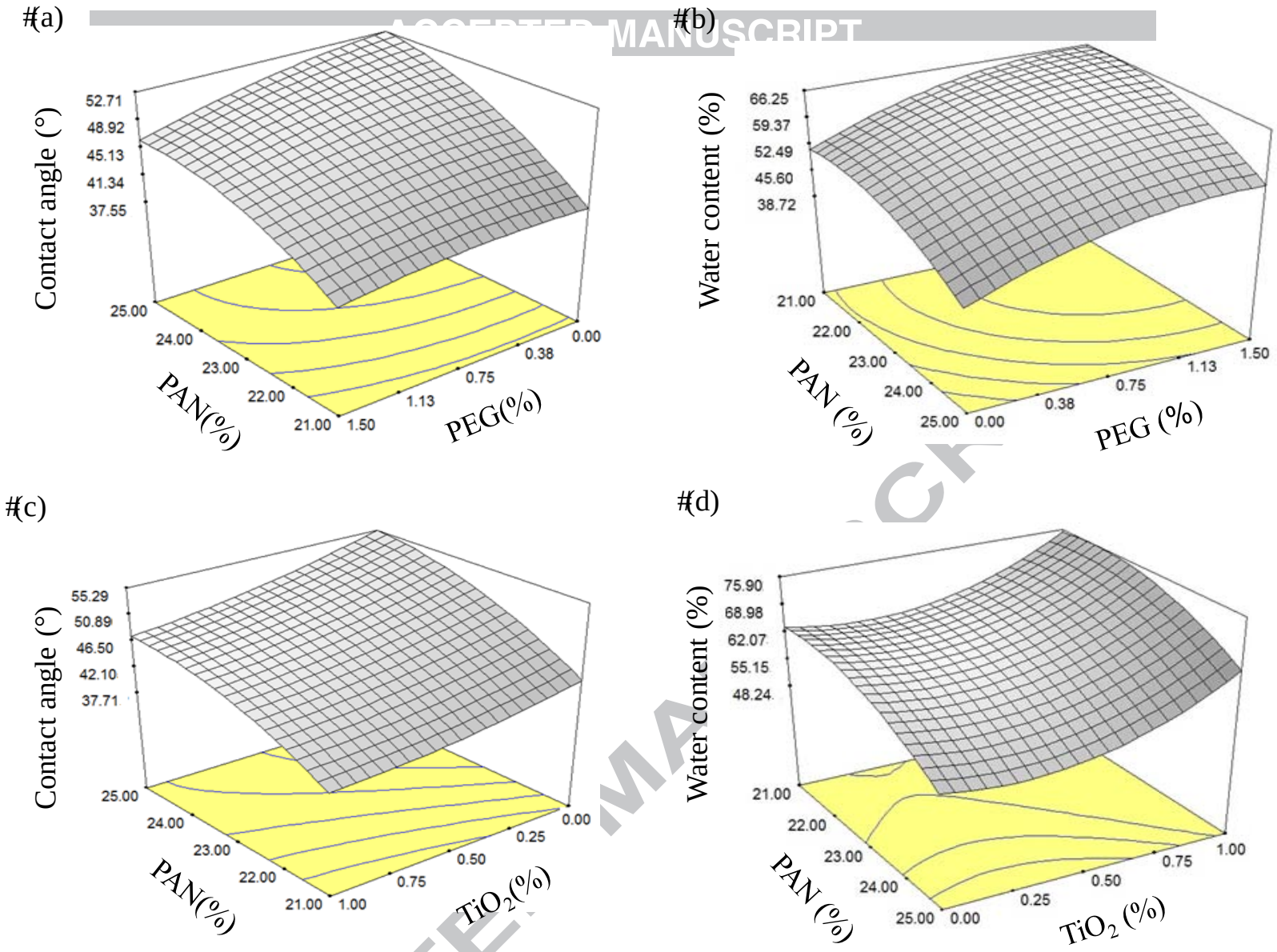

Fig. 4. Individual effects of of PEG (a &b) and TiO_2 (c &d) concentration on the contact angle and water contents of membranes.

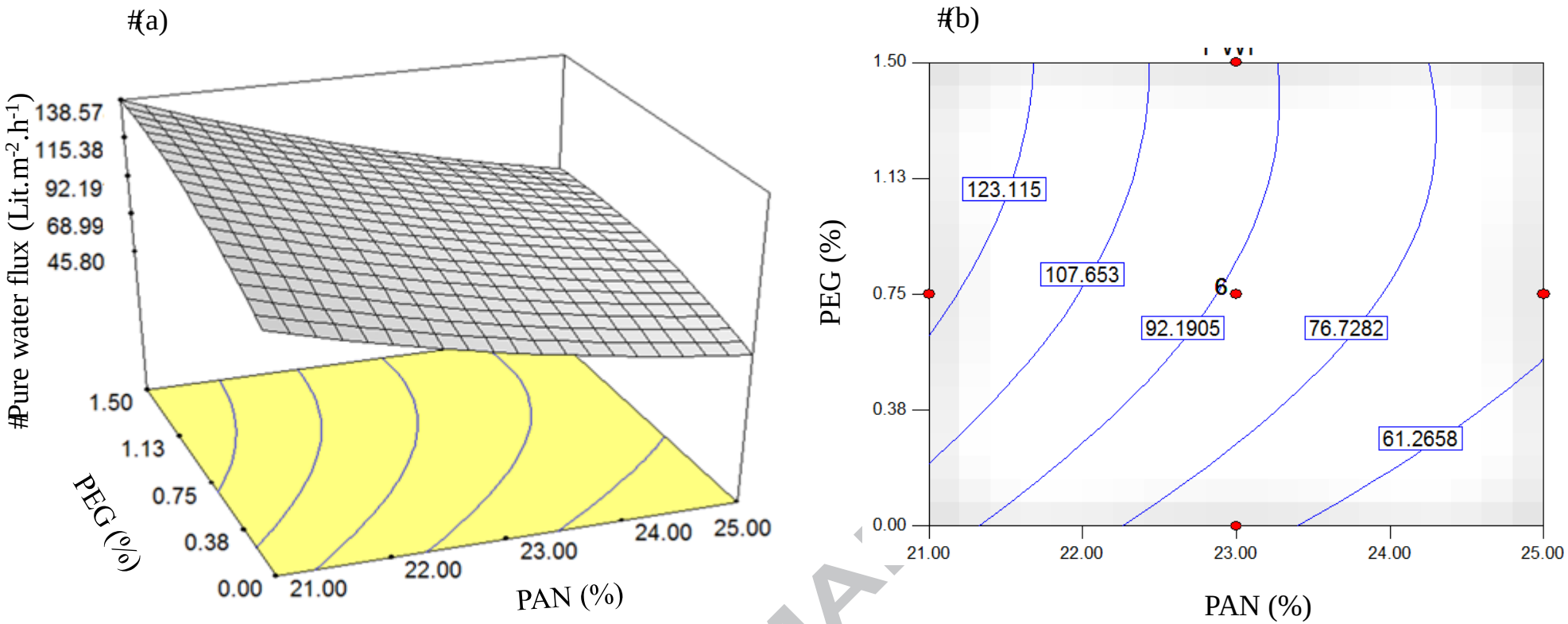

Fig. 5. Response surface for the effect of PAN and PEG concentration on pure water flux (a) 3D surface (b) Contour. (TiO_2 conc.: 0.5 wt.%)

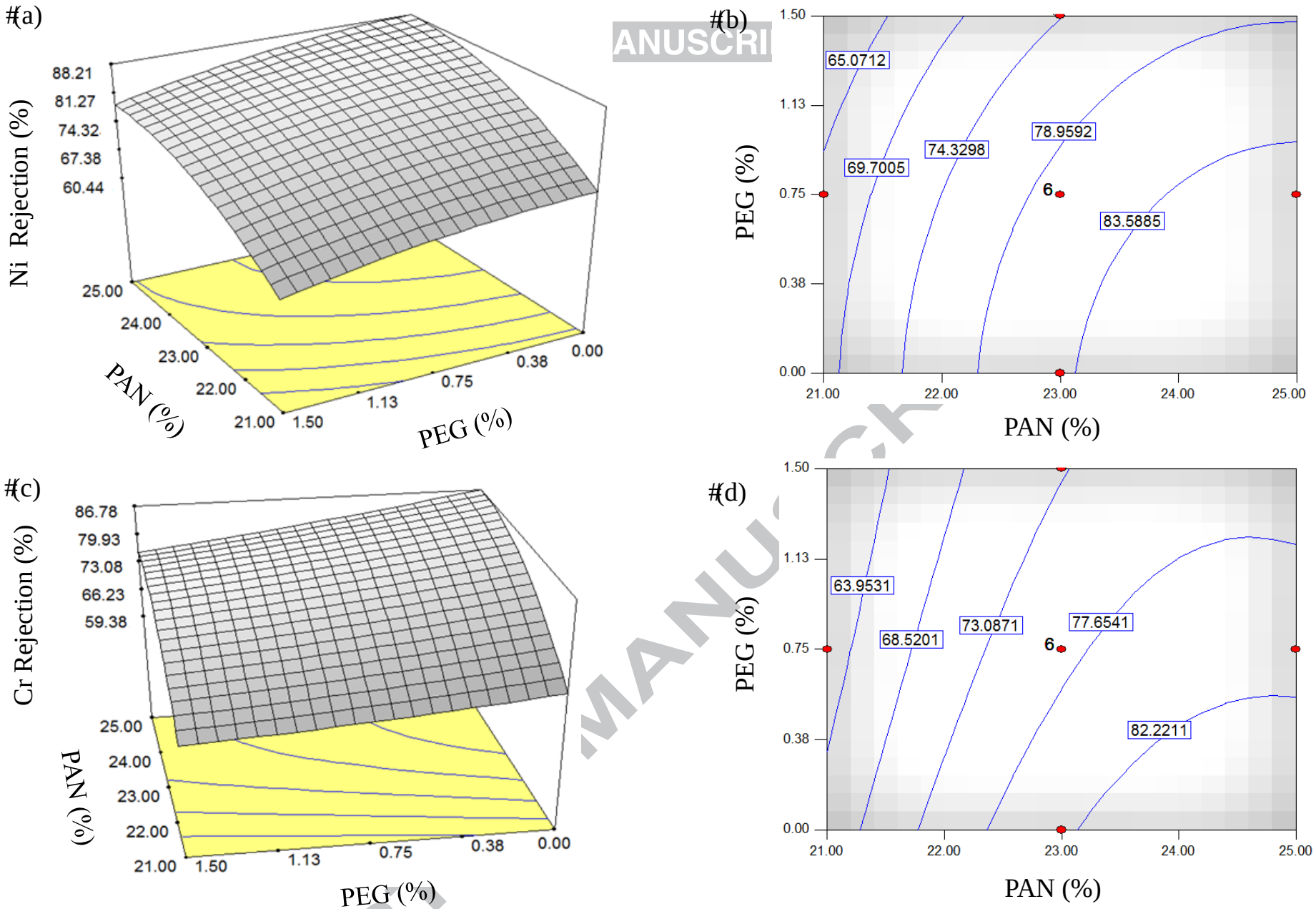

Fig. 6. Response surface for the effect of PAN and PEG concentrations on Ni rejection (a) 3D surface (b) Contour and Cr rejection (c) 3D surface (d) Contour. (Membranes contain 0.5 wt.% TiO_2)

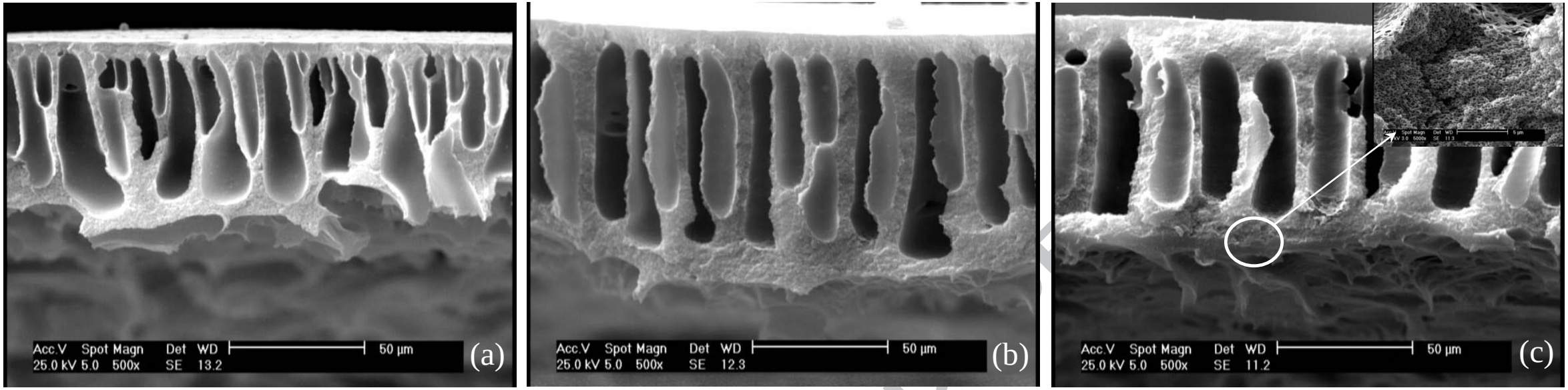

Fig. 7. The effect of PEG concentration in dope on the morphology of NF membranes (a) PEG: 0 wt.% (b) PEG: 0.75 wt.% (c) PEG: 1.5 wt.% (conditions: PAN Conc.: 23 wt.%, TiO_2 Conc. 0.5 wt.%, solvent: DMF, coagulating agent: water, coagulation bath temperature: 25 ˚C, casting knife gap: 200 µm).

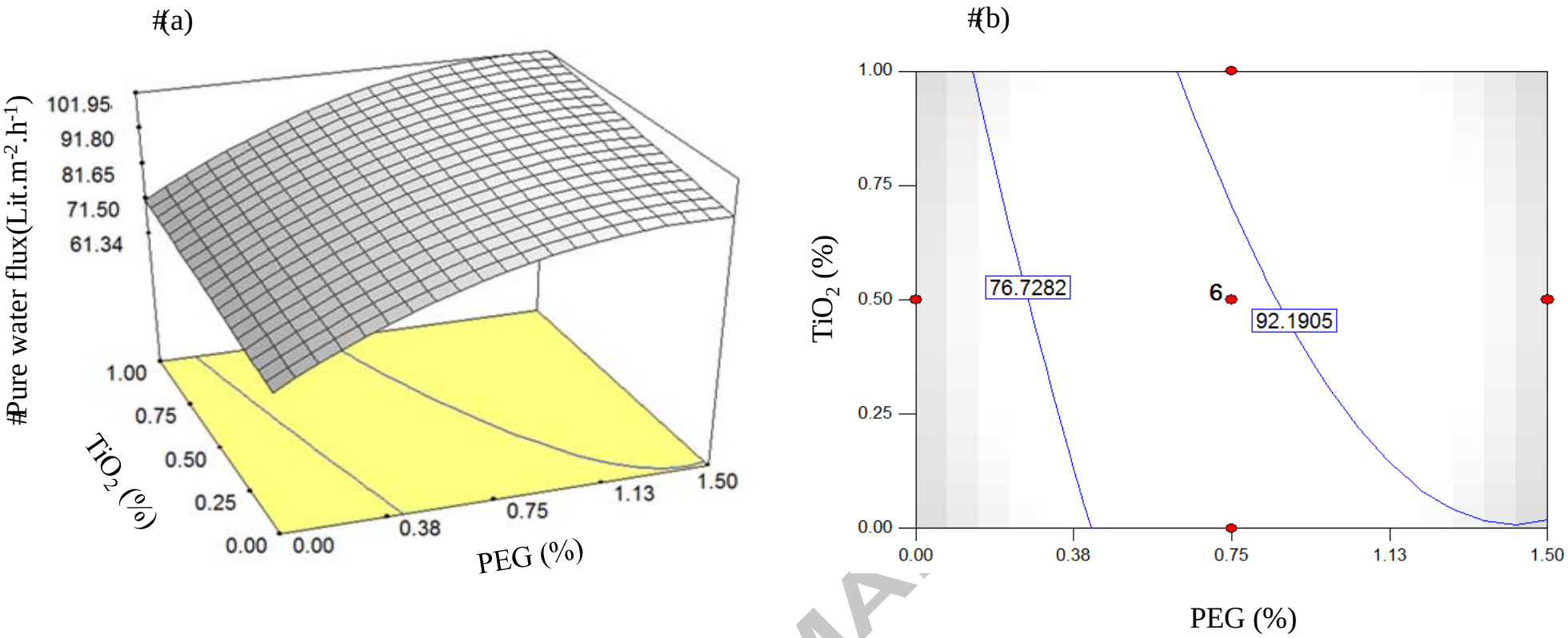

Fig. 8. Response surface for the effect of PAN and PEG concentration on pure water flux (a) 3D surface (b) Contour. (PAN conc.: 23 wt.%)

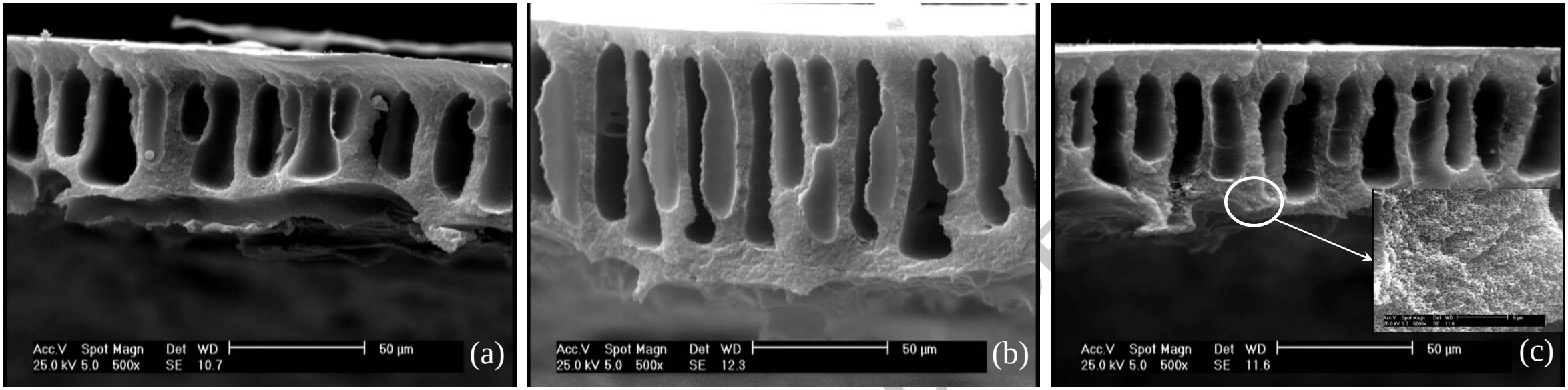

Fig. 9. The effect of TiO_2 concentration in dope on the morphology of NF membranes (a) TiO_2: 0 wt.% (b) TiO_2: 0.5 wt.% (c) TiO_2: 1 wt.% (conditions: PAN Conc.: 23 wt.%, PEG Conc. 0.75 wt.%, solvent: DMF, coagulating agent: water, coagulation bath temperature: 25 ˚C, casting knife gap: 200 µm).

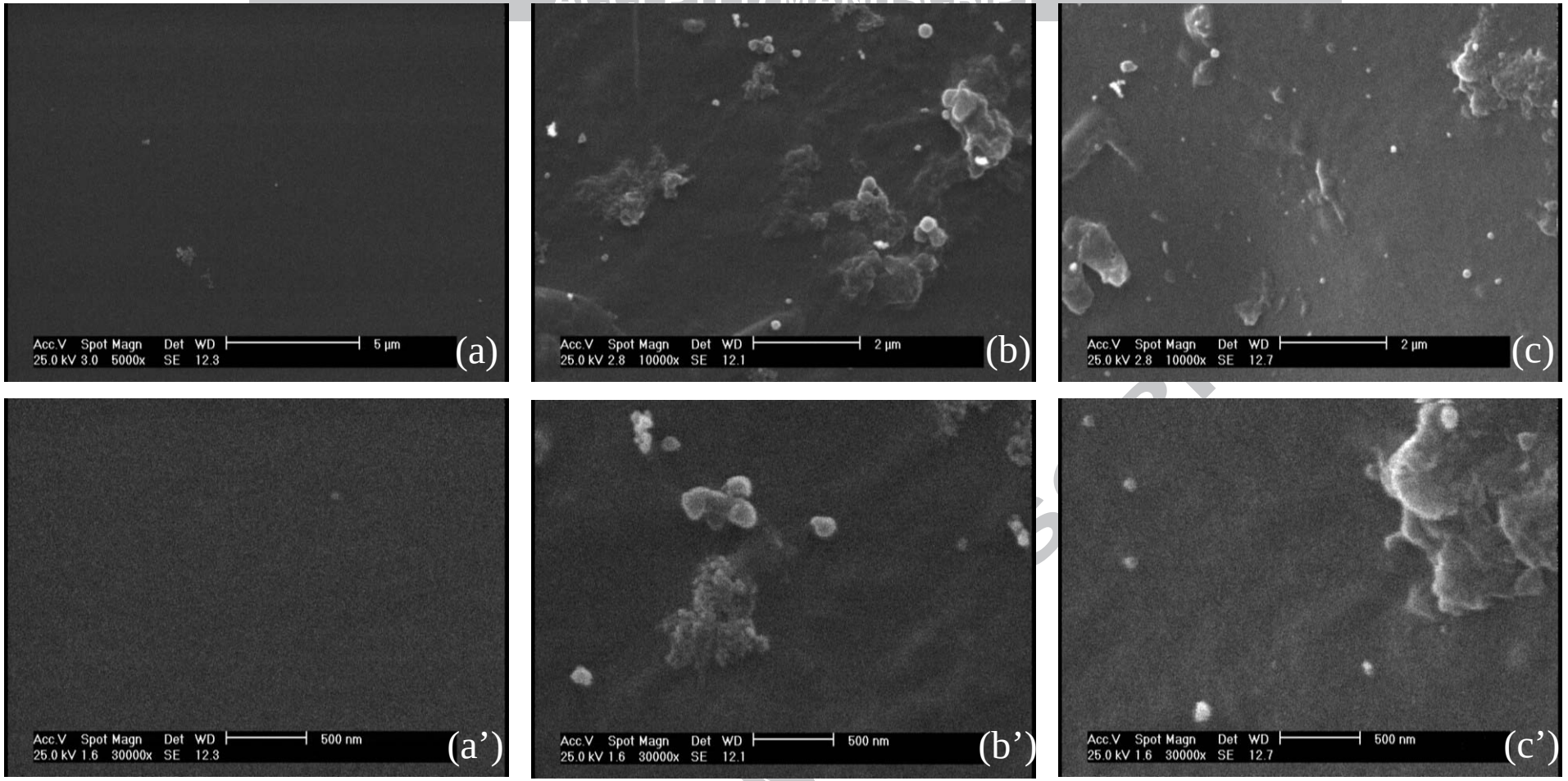

Fig. 10. The effect of addition of PEG, TiO_2 and combined PEG-TiO_2 on the surface morphology of NF membranes (a&a') PEG: 0.75 wt.% TiO_2: 0 wt.% (b&b') PEG: 0 wt.% TiO_2: 0.5 wt.% (c&c') PEG: 0.75 wt.% TiO_2: 0.5 wt.% (conditions: PAN Conc.: 23 wt.%, solvent: DMF, coagulating agent: water, coagulation bath temperature: 25 ˚C, casting knife gap: 200 µm).

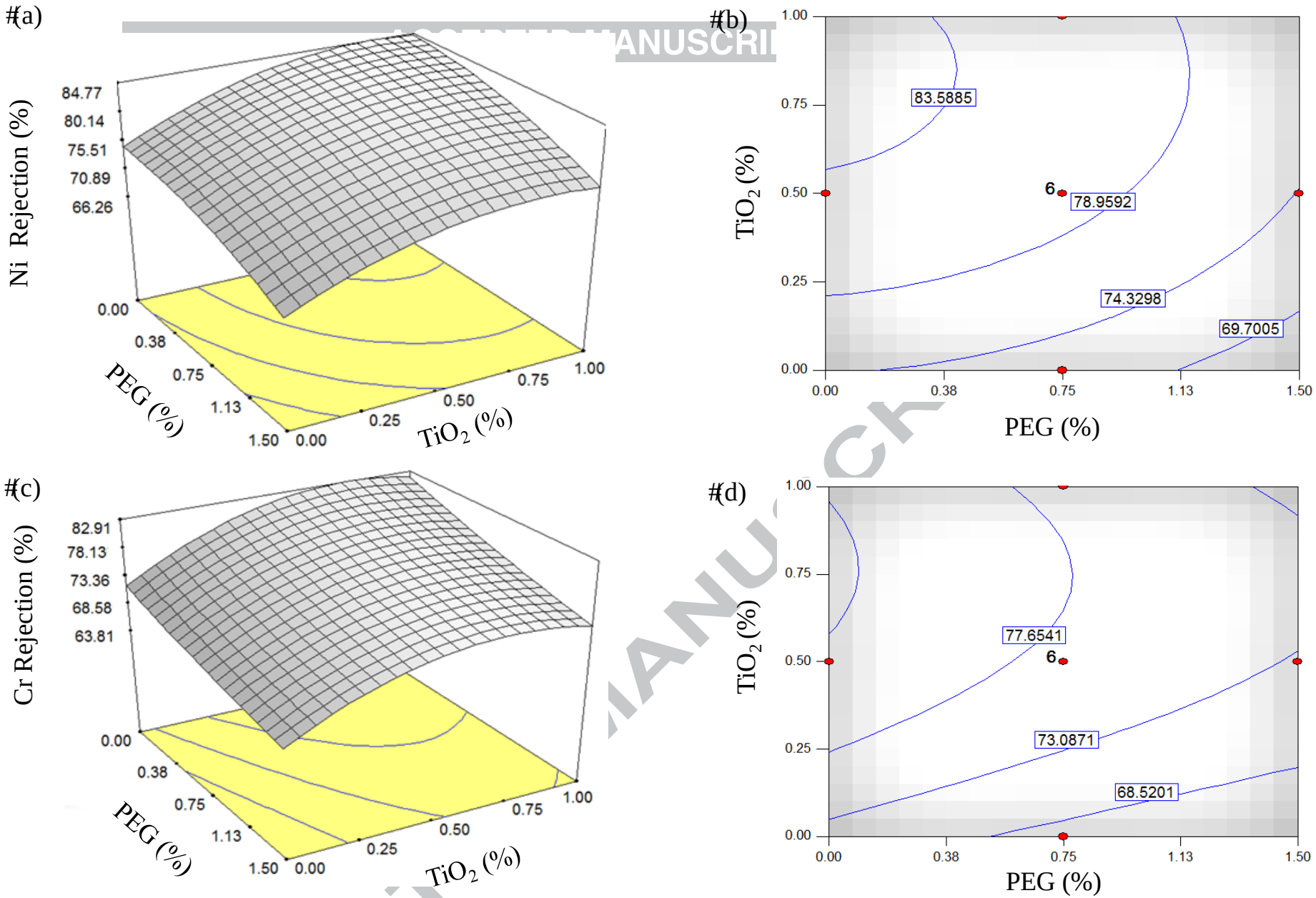

Fig. 11. Response surface for the effect of PEG and TiO_2 concentrations on Ni rejection (a) 3D surface (b) Contour and Cr rejection (c) 3D surface (d) Contour. (PAN conc.:23%)

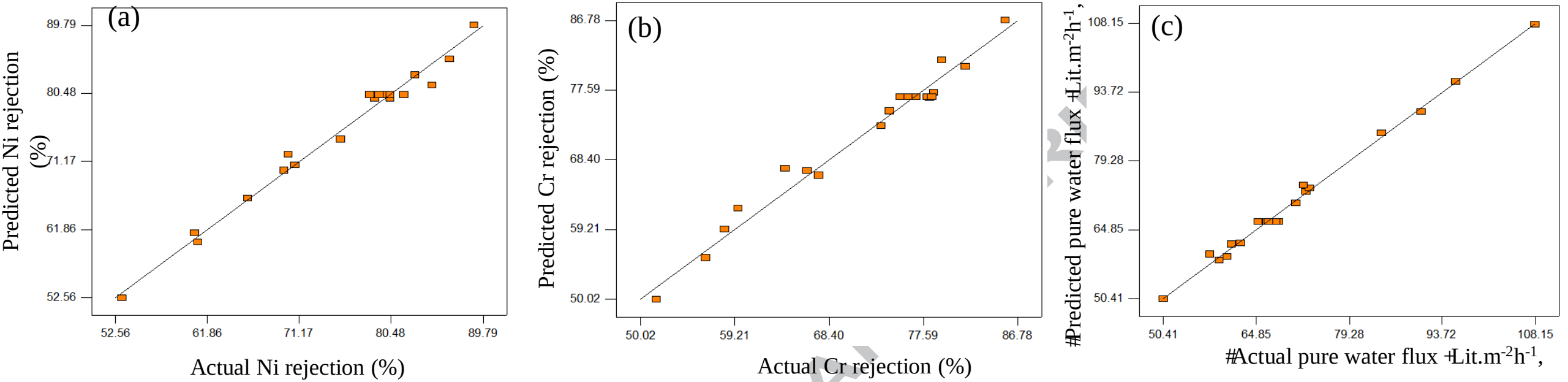

Fig. 12. Comparison between experimental (actual) and predicted value for (a) Ni rejection, (b) Cr rejection and (c) pure water flux.

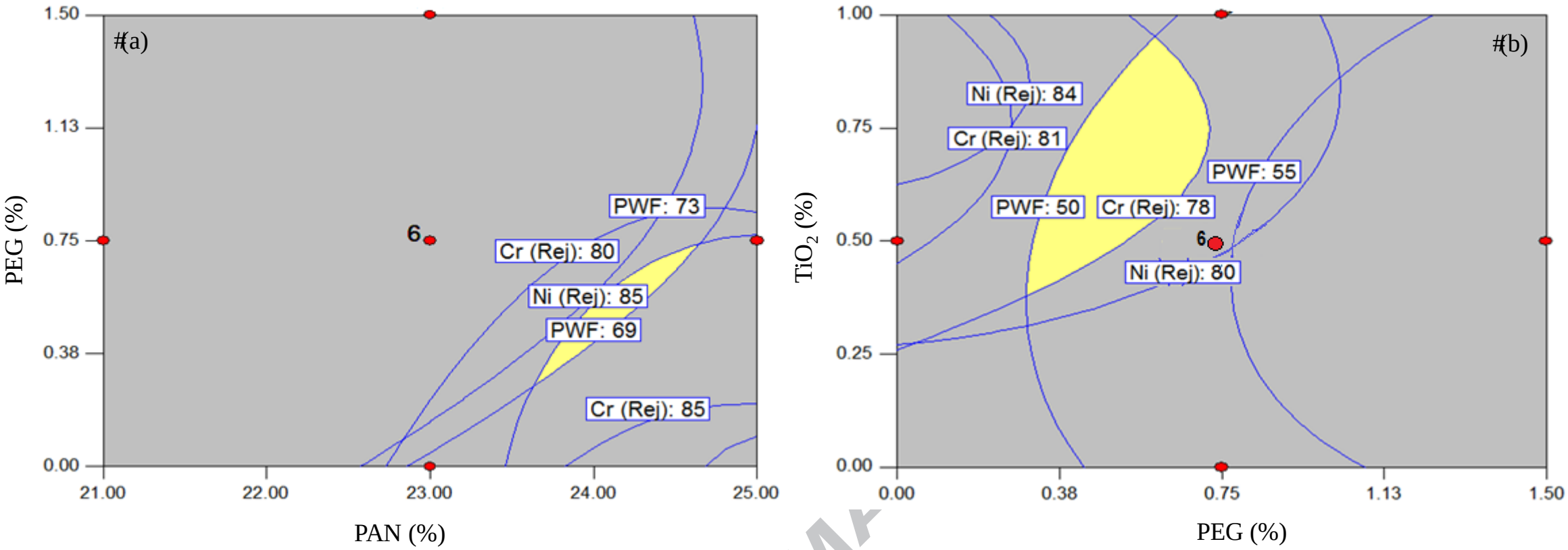

Fig. 13. The optimum region by overlaying plot of the three responses evaluated as a function of PAN, PEG and TiO_2 concentration (%) (a) at constant TiO_2=0.5% (b) at constant PAN=23%.

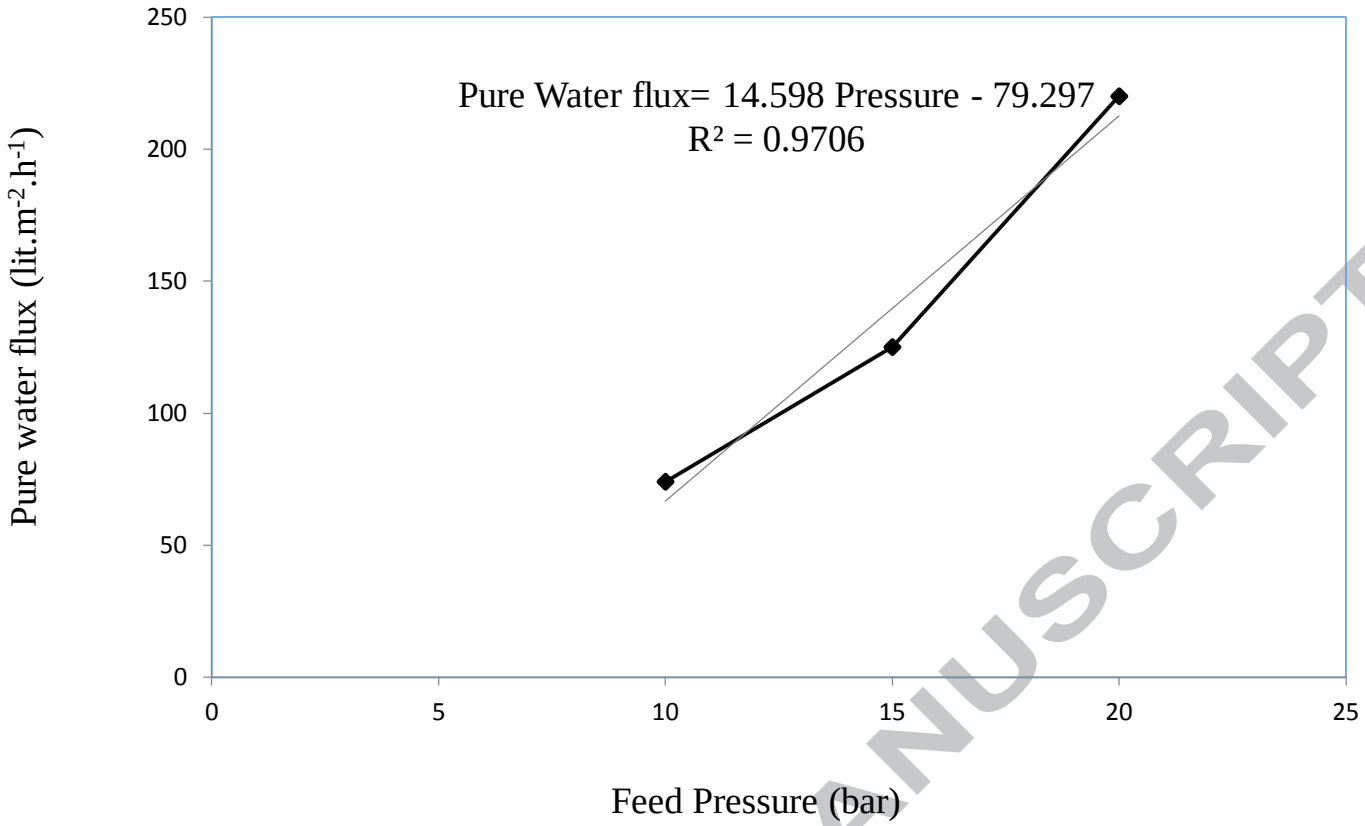

Fig. 14. The effect of feed pressure on pure water flux for optimized membrane (PAN: 23.91%, PEG: 0.41%, TiO_2: 0.82%).

Table 1.The properties of TiO_2 nanoparticles used in this study.

Properties	**Specification**
Titanium Oxide Nanoparticles	TiO_2, rutile
Purity	99.9+%
APS	30 nm
SSA	35-60m^2/g
Color	white
Morphology	spherical
True density	4.23 g/cm^3

Table 2. List of independent variables and their levels.

Variable	Low factorial (-1)	Central (0)	High factorial (+1)
Poly(acrylonitrile) (wt.%)	21	23	25
Poly(ethylene glycol) (wt.%)	0	0.75	1.5
Titanium dioxide (wt.%)	0	0.5	1

Sample/ Run	Variables in coded levels			Responses		
	PAN (%)	PEG (%)	TiO_2 (%)	Pure Water flux ($Lit.m^{-2}.h^{-1}$)	Ni Rejection (%)	Cr Rejection (%)
1	-1	-1	-1	94.86	60.87	56.35
2	-1	0	0	123.12	65.93	59.53
3	0	0	-1	84.28	70.06	64.12
4	-1	1	-1	132.31	53.21	51.57
5	0	0	0	87.31	79.26	77.99
6	-1	-1	1	104.57	69.63	67.39
7	0	0	0	90.23	80.12	78.21
8	0	0	0	88.01	78.32	78.44
9	1	1	-1	59.86	70.75	66.27
10	0	0	1	93.97	84.64	78.24
11	0	0	0	91.42	80.36	76.92
12	0	-1	0	65.40	82.88	79.42
13	1	0	0	71.22	86.39	81.71
14	0	0	0	92.59	81.78	75.36
15	1	1	1	69.47	78.81	74.32
16	0	0	0	91.19	79.72	76.13
17	1	-1	1	48.14	88.87	85.60
18	1	-1	-1	41.35	80.36	78.64
19	0	1	0	100.29	75.36	73.51
20	-1	1	1	145.72	60.57	58.21

Table 3. The list of the samples and their corresponding variables and responses derived based on the experimental design.

Table 4. Effect of PAN concentration on porosity and mean pore size of the membranes.

Sample/ Run	PAN (%)	PEG (%)	TiO_2 (%)	Porosity (%)	Mean pore size (nm)
1	21	0	0	59.44	10.15
18	25	0	0	44.41	7.99

Table 5. Effect of PEG and TiO2 concentration on the characteristics of NF membranes.

Sample/ Run	PAN (%)	PEG (%)	TiO_2 (%)	Thickness (µm)	Porosity (%)	Mean pore size (nm)	Area fraction of macro-voids
12	23	0	0.5	167.44	56.15	8.59	49.8
5	23	0.75	0.5	178.83	65.21	9.31	50.7
19	23	1.5	0.5	181.32	74.93	9.73	54.9
3	23	0.75	0	170.13	56.74	9.76	48.1
5	23	0.75	0.5	178.83	65.33	9.31	49.8
10	23	0.75	1	165.15	73.39	8.21	46.9

Source	DF	Ni Rejection (%)			Cr Rejection (%)			Pure water flux (Lit.m^{-2}.h^{-1})		
		Coefficient	Sum of squares	p-value	Coefficient	Sum of squares	p-value	Coefficient	Sum of squares	p-value
Model	9	-651.445	1677.91	<0.0001	-757.999	1674.26	<0.0001	1195.563	12680.61	<0.0001
Linear										
PAN	1	58.228	901.93	<0.0001	66.700	874.04	<0.0001	-85.945	9643.51	<0.0001
PEG	1	4.579	192.81	<0.0001	11.938	189.40	<0.0001	114.859	2351.01	<0.0001
TiO_2	1	22.410	223.45	<0.0001	36.931	219.12	<0.0001	34.230	242.16	0.0006
Quadratic										
PAN^2	1	-1.159	59.13	0.0010	-1.331	78.02	0.0017	1.593	111.60	0.0073
PEG^2	1	2.981	7.73	0.1281	0.992	0.74	0.6876	-14.141	174.01	0.0019
TiO_2^2	1	-13.787	32.67	0.0067	-19.065	62.48	0.0035	-6.699	7.71	0.3986
Interaction										
PAN										

Table 7. Predicted optimum condition for removal of Ni and Cr from wastewater

Factor	Low	High	Optimum
PAN (%)	21	25	23.93
PEG (%)	0	1.5	0.41
TiO_2 (%)	0	1	0.82

Table 8. Performance data for several commercial and non-commercial NF membranes

Membrane type	Water flux ($Lit.m^{-2}.h^{-1}$)	Ni rejection (%)	Cr rejection (%)	Operating conditions	Ref.
Poly(acrilonitryle) (PAN/PEG/TiO2:23.93/0.41/0.82, wt.%)	71.8	87.0	83.2	P = 10 bar	Present study
NF-90	52, 54 (Ni, Cr)	99.2	96.5	P = 30 bar	[83]
NF-270	69, 224 (Ni, Cr)	98.7	95.7		
AFC30	35	75	75	P = 15 bar	[84]
AFC40	55				
Polyamide TFC	47.5	95.7	94.9	P = 4 bar	[85]
Chelating polymer modified P84	~ 10	> 98	> 98	P = 10 bar	[81]
NF-300	~ 70	~ 60	~ 55	P = 8 bar	[86]

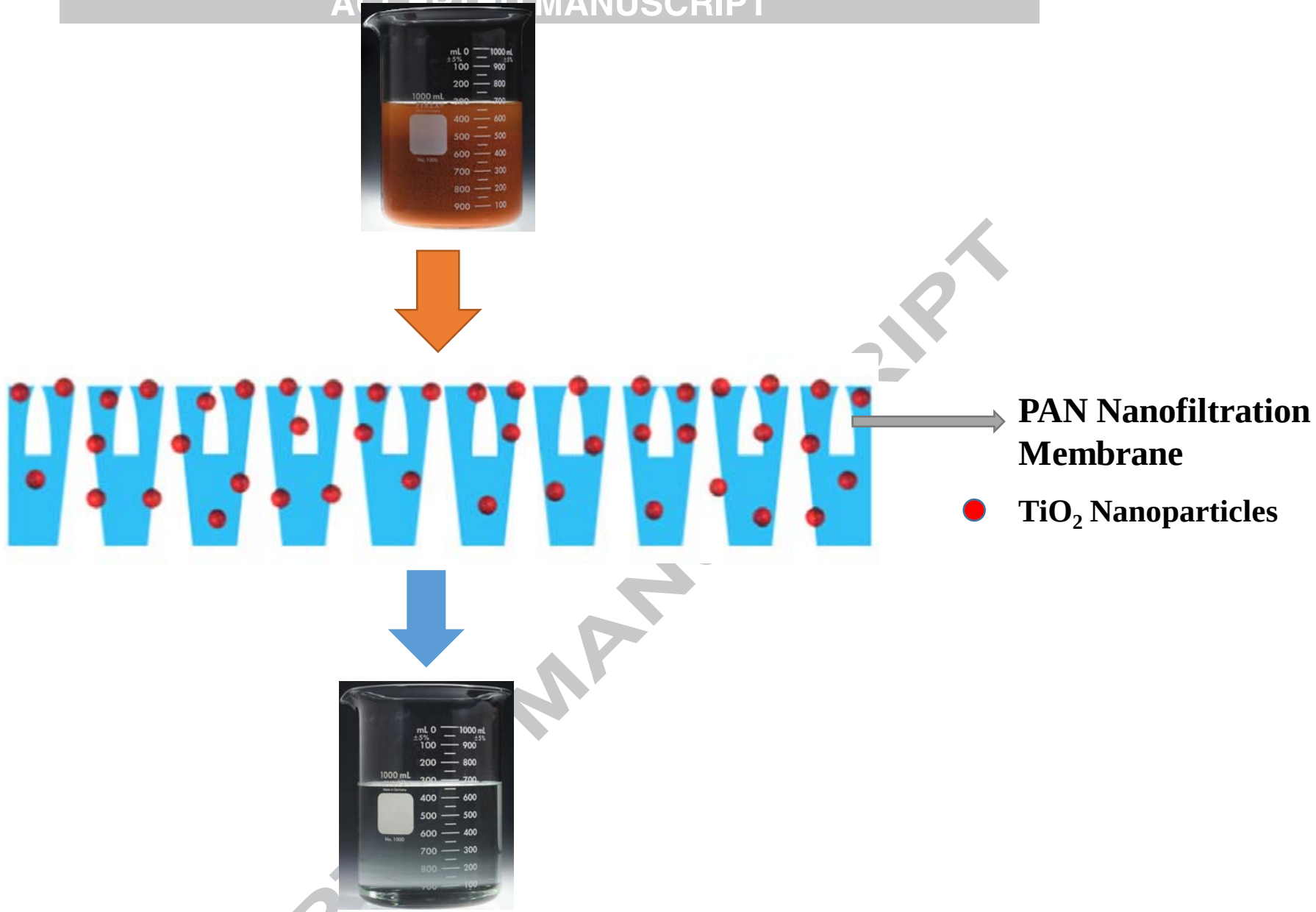

Research Highlights:

PAN nanofiltration membranes are designed and fabricated by phase inversion process

Performance of developed membranes are tested for electroplating wastewater treatment

Effects of addition of TiO_2 nanoparticles and PEG on the performance are investigated

Response surface method used for optimization of membrane structure and performance

Developed membranes show satisfactory performance compared to other NF membranes